Distributions and accumulation mechanisms of helium in petroliferous basins

Pengpeng Li[1], Quanyou Liu[1,2,*], Dongya Zhu[3], Di Zhu[4], Zheng Zhou[5], Xiaoqi Wu[3], Qingqiang Meng[3], Jiaohao Lv[6,7], Yu Gao[1]

[1] *Institute of Energy, Peking University, Beijing 100871, China;*
[2] *Northwest Institute of Eco-Environment and Resources, Chinese Academy of Sciences, Lanzhou 730000, China;*
[3] *Petroleum Exploration & Production Research Institute, SINOPEC, Beijing 102206, China;*
[4] *Energy Research Institute, Qilu University of Technology (Shandong Academy of Sciences), Jinan 250014, China;*
[5] *Lancaster Environment Centre, Lancaster University, LA1 4YQ, UK;*
[6] *Institute of Geology and Geophysics, Chinese Academy of Sciences, Beijing 100029, China*
[7] *University of Chinese Academy of Sciences, Beijing 100049, China*
* Corresponding author: (liuqy@pku.edu.cn; qyouliu@sohu.com)

Abstract: Helium is an irreplaceable strategic mineral resource, and commercial helium-rich gas fields (He>0.1%) worldwide are typically discovered serendipitously during hydrocarbon exploration efforts. According to an analysis of 75 helium-rich gas fields and 1048 natural gas samples worldwide, helium in natural gas generally exhibits "scarce", "accompanying", and "complex" properties, and helium-rich gas fields often occur at depths <4500 m. Helium concentrations in He-CH_4 and He-CO_2 gas fields are notably lower than those in He-N_2 gas fields (He>1%). However, geological reserves in the former two types of gas fields are mainly in the range of 10^7–10^{11} m^3, whereas in the latter, they are only in the range of 10^5–10^7 m^3. There are nevertheless notable disparities in the genesis and migration patterns between helium and gaseous hydrocarbons. Helium necessitates carriers (such as formation water, hydrocarbon fluids, N_2, mantle-derived fluids, etc.) during both accumulation and long-distance migration processes, where migration conduits are not confined to sedimentary strata, and may extend to the basin's basement, lower crust, and even lithospheric mantle. However, the accumulation conditions of both helium and gaseous hydrocarbons are generally considered equivalent. The presence of gaseous hydrocarbons facilitates both the rapid exsolution of helium within helium-containing fluids and subsequent efficient aggregation in gaseous hydrocarbons, while both reduce helium diffusion and diminish escape flux. In terms of caprock, gypsum, salt, and thick shale as sealing layers contribute to the long-term preservation of helium over geological timescales. Large helium-rich gas fields, predominantly crust-derived gas fields, are primarily concentrated in uplifted zones of ancient cratonic basins and their peripheries. Based on a diagram of the He concentration versus He/N_2 ratio, crust-derived helium fields can be categorized as basement, combined basement-sedimentary rock, and sedimentary rock helium supply types. Comprehensively given China's helium grade, helium resource endowment, natural gas industrialization process, and current helium purification processes, the foremost deployment zones for the commercial production of helium should be the helium-rich gas fields located in the Ordos, Tarim, Sichuan, and Qaidam Basins in western and central China. In addition, certain (extra) large helium-containing gas fields serve as important replacement zones.

Keywords: Helium resource; Geochemical characteristics; Helium source rock, Helium supply pattern; Accumulation mechanism; Determination of favorable zones

1 Introduction

Helium is a known element that has the lowest boiling point temperature in nature. Due to its low density and enhanced inertness, helium has become an irreplaceable and scarce strategic resource for development of high-tech manufacturing and key scientific and technological fields (Broadhead, 2005; Cai et al., 2010; Anderson, 2018). Helium resources are distributed extremely unevenly around the globe and are mainly concentrated in certain countries, such as the United States, Qatar, Algeria, and Russia. Moreover, since the beginning of this century, contradictions between supply and demand in the international helium market have become increasingly prominent, highlighting the significance of strategic considerations regarding helium resources.

China lacks strategic reserves of helium, leading to a heavy reliance on imports for helium resources, with more than 90% dependence on external sources for a long time. Moreover, the rapid development of high-tech industries, national defense, and aerospace sectors in China has resulted in an annual growth rate of helium demand of approximately 10% (Zhao et al., 2012; Anderson, 2018). In this regard, since 2017, the annual helium consumption in China has remained above 20×10^6 m^3, even reaching 24.04×10^6 m^3 in 2022. It is anticipated to continue growing for an extended period. The Weiyuan gas field was discovered in 1964 and is known as the first industrial base for helium extraction in China. After nearly 60 years of extraction, due to the depletion of natural gas resources, the current annual helium production is only 30000 to 70000 m^3 (Li Y H et al., 2018). Since 2020, relevant departments in China have been actively building the infrastructure for helium production, leading to a domestic helium production of 1.95×10^6 m^3 in 2022. However, compared to helium consumption, there is still a significant gap in the demand for helium. China currently lacks an independent helium extraction industry, and new technologies are currently in the stage of exploration and technological breakthrough. Consequently, it is impossible to overcome this difficulty in the short term–the helium will remain highly dependent on imports in the near future. In recent years, major helium-producing countries, notably led by the United States, have enacted laws to safeguard helium resources, and have imposed restrictions on the export of crude helium. This tight control over the helium market has resulted in a surge in the price of liquid helium and a contraction in the helium trade globally (Broadhead, 2005; Cai et al., 2010; Anderson, 2018). This poses a serious threat to the security of China's helium resource supply and its critical strategic needs. Therefore, it is imperative to assess the distribution and potential of domestic helium resources and to expedite the exploration and development of helium accordingly (Li Y H et al., 2018; Tao et al., 2019; Chen et al., 2021; Li et al., 2022; Peng et al., 2022).

Helium, commonly as a trace component, is accompanied by varying amounts of natural gas (CH_4, CO_2, N_2, H_2) in different geological settings, such as mid-ocean ridges, volcanic craters, geothermal fluids, hot springs, sedimentary basins (Xu et al., 1998; Ballentine and Burnard, 2002; Brown, 2010; Keir, 2010; Guélard et al., 2017; Xu et al., 2014; Han et al., 2022; Ranta et al., 2023). However, extracting helium from natural gas is currently the only economically viable option (Anderson, 2018; Liu Q Y et al., 2022; Peng et al., 2022). It is widely accepted that natural gas containing helium at concentrations ranging from 0.05% to 0.1% has helium extraction potential (Xu et al., 1996), when the helium concentration surpasses 0.3%, it is considered to have exceptionally high industrial extraction value (Danabalan, 2017). According to statistical analysis of helium concentrations in natural gas from major petroliferous basins in China, Dai et al. (2017) proposed that gas fields could be divided into helium-extremely rich (≥0.500%), helium-rich (0.150–0.500%), helium-generally rich (0.050–0.150%), helium-depleted (0.005–0.050%), and helium-extremely depleted (<0.005%) types. Moreover, gas fields can be divided into extra-large ($\geq100\times10^6$ m^3), large (50×10^6–100×10^6 m^3), medium (25×10^6–50×10^6 m^3), small (5×10^6–25×10^6 m^3), and very-small ($<5\times10^6$ m^3) types, according to their helium reserves. Chen et al. (2021) proposed a different scheme in which natural gases are divided into helium-depleted (<0.05%), helium-containing (0.05%–0.10%), and helium-rich (≥0.10%) categories according to their helium concentration. Therefore, in this study, the scheme for assessing the helium concentration in natural gas followed Chen et al. (2021), while the framework for characterizing the helium gas field was based on the approach proposed by Dai et al. (2017).

Exploration activities have revealed various types of helium resources in multiple petroliferous basins in China. For example, "crust-mantle-complex-type" helium resources are mainly distributed in periphery of the Tancheng-Lujiang Fault Zone in eastern China (Xu et al., 1994, 1997a, 1997b; Tao et al., 1997; Zheng et al., 2001; Dai et al., 2005; Feng et al., 2008; Wang et al., 2023), whereas "crust-type" helium resources are mainly distributed in the central and western cratonic basins (Tao et al., 2019; Zhang et al., 2020; He F Q et al., 2022; Peng et al., 2022). The Dongsheng gas field in the Ordos Basin and the Hetianhe gas field in the Tarim Basin are extra-large helium-rich fields. In addition, helium concentration in marine shale gas from the Wufeng-Longmaxi Formations in the Sichuan Basin, as well as its periphery, is approximately 0.04%. Although the helium concentration is relatively low, proven helium reserves are very significant, with a preliminary assessment of up to 10.8×10^8 m^3 (Nie et al., 2023), making it an extra-large and helium-depleted gas field. These helium reserves are vital for meeting the need for the domestic use of helium.

Helium-rich gas fields with commercial potential (mainly alkane gas fields) have all been discovered serendipitously during petroleum exploration activities (Danabalan, 2017), such as in the Hugoton-Panhandle gas field in the United States, and the Weiyuan, Hetianhe, and Dongsheng gas fields in China. During previous petroleum explorations, helium was not considered an independent mineral resource for exploration and development, therefore, the distribution and resource potential of helium are unclear. In this regard, some works have attempted to use noble gas isotopes to trace the migration and accumulation of helium-containing geological fluids, as well as the filling periods of hydrocarbon fluids (Elliot et al., 1993; Ballentine and Sherwood Lollar, 2002; Barry et al., 2016, 2017; Byrne et al., 2018; Zhang et al., 2019a, 2019b, Danabalan et al., 2022; Halford et al., 2022). Despite of these efforts, specific research on the key factors associated with helium accumulation, the primary factors influencing its enrichment, and its accumulation models remain elusive. To address this gap, we compiled the geochemical characteristics of helium-rich gas fields, analyzed the key components contributing to helium accumulation, and explained the principal factors governing on helium enrichment in natural gas. With these goals, this work provides a reference for developing theories on helium enrichment and accumulation, evaluating the helium resource potential, and guiding the future deployment of commercial helium extraction.

2 Global distributions of helium resources

The distributions of helium resources around the globe are shown in Table 1. As of the end of 2021, the global helium resources were approximately 484×10^8 m^3 (USGS, 2022). The United States has the largest amount of helium resources in the world, at 171×10^8 m^3, accounting for 35% of the total. Qatar, Algeria, Russia, and Canada have helium resources of 101×10^8 m^3, 82×10^8 m^3, 68×10^8 m^3, and 20×10^8 m^3, respectively accounting for 21%, 17%, 14%, and 4% of the global helium resources, respectively (USGS, 2022).

The helium recoverable reserves are estimated to be 120.86×10^8 m^3 worldwide, with the United States having the highest helium recoverable reserves (85.61×10^8 m^3), followed by Algeria (18×10^8 m^3) and Russia (17×10^8 m^3) (USGS, 2022). Therefore, these three countries account for 99.99% of the global recoverable reserves of helium. Although Qatar is the world's second largest helium supplier following the United States, its helium is generally purified and subsequently recovered through liquefied natural gas- boiled off gas (LNG-BOG) due to the low helium concentration in the North Pars gas field (only approximately 0.04%). Therefore, helium recoverable reserves in Qatar are not incorporated into the USGS statistical sheets. Ultimately, most other countries have not yet conducted exploration or thorough assessment of their helium resources, leaving their potential largely unknown.

Since the early 2000s, as mentioned earlier, governments worldwide have enacted laws to protect helium resources due to persistent supply-demand imbalances in the global helium market. In response, certain companies with experience in petroleum or mineral exploration, as well as start-ups, have initiated exploration activities that specifically target helium. With these efforts, new resources have been discovered, therefore, the global distribution of helium has changed. For example, in 2017, the Helium One Company discovered abundant helium resources in the Rukwa, Eyasi, and Balangida Basins/regions in Tanzania, with a preliminary estimate of helium recoverable reserves (P_{50}) in the Rukwa Basin of approximately 27.8×10^8 m^3 (Danabalan et al., 2022). Likewise, during 2019–2022, two helium rich gas fields (Hetianhe and Dongsheng) were also discovered in China (Tao et al., 2019; Peng et al., 2022), with a preliminary assessment of helium recoverable reserves in these two gas fields of approximately 2.2×10^8 m^3 (the Hetianhe and Dongsheng gas fields have natural gas recovery efficiencies of 62% and 40%, respectively).

Table 1 Distributions of helium resources worldwide

Nation	Helium resources (10^8 m^3)	Helium recoverable reserves (10^8 m^3)	Helium proved reserves in the past five years (10^8 m^3)
United States*	171	85.51	no data
Qatar*	101	no data	no data
Algeria*	82	18	no data
Russia	68	17	no data
Canada	20	no data	no data
Tanzania	no data	no data	27.8 (P_{50})

China	11	no data	2.2

*: Major helium suppliers worldwide

3 Geochemical characteristics of helium

Statistical analysis of geochemical data from natural gas samples collected from major petroliferous basins worldwide indicates that helium in natural gas generally exhibits "scarce", "accompanying", and "complex" properties. These geochemical characteristics suggest that objectively, understanding the migration and enrichment patterns of helium, elucidating the accumulation mechanisms of helium, and predicting helium resource targets are challenging endeavors.

3.1 “Scarce”: Helium has a low concentration in natural gas

Throughout the world, the helium concentration in natural gas is generally low, with most being well below the level at which it can be easily extracted for commercial use (0.1%). Based on experimental data obtained from 1048 natural gas samples, 768 samples had helium concentrations below 0.1%, accounting for approximately 73.3% of the total number of samples. Among these samples, 245, 364, and 159 had helium concentrations less than 0.02%, between 0.02% and 0.05%, and between 0.05% and 0.1%, respectively. There were 217 samples with helium concentrations ranging from 0.1% to 0.3%, accounting for 20.7% of the total number of samples. Furthermore, only 63 samples had helium concentrations exceeding 0.3%, which is approximately 6.0% of the total samples (Figure 1a). This indicates that the formation of a helium-rich gas field requires helium that is unusually concentrated in the gas. However, the dynamic diameter of the helium molecule is only 0.26 nm, and the helium molecule has a strong diffusion ability, thus, excellent preservation conditions are required for commercial accumulation in the subsurface. Therefore, understanding the conditions under which helium can be highly concentrated in petroliferous basins is crucial for understanding the mechanisms of helium enrichment and accumulation.

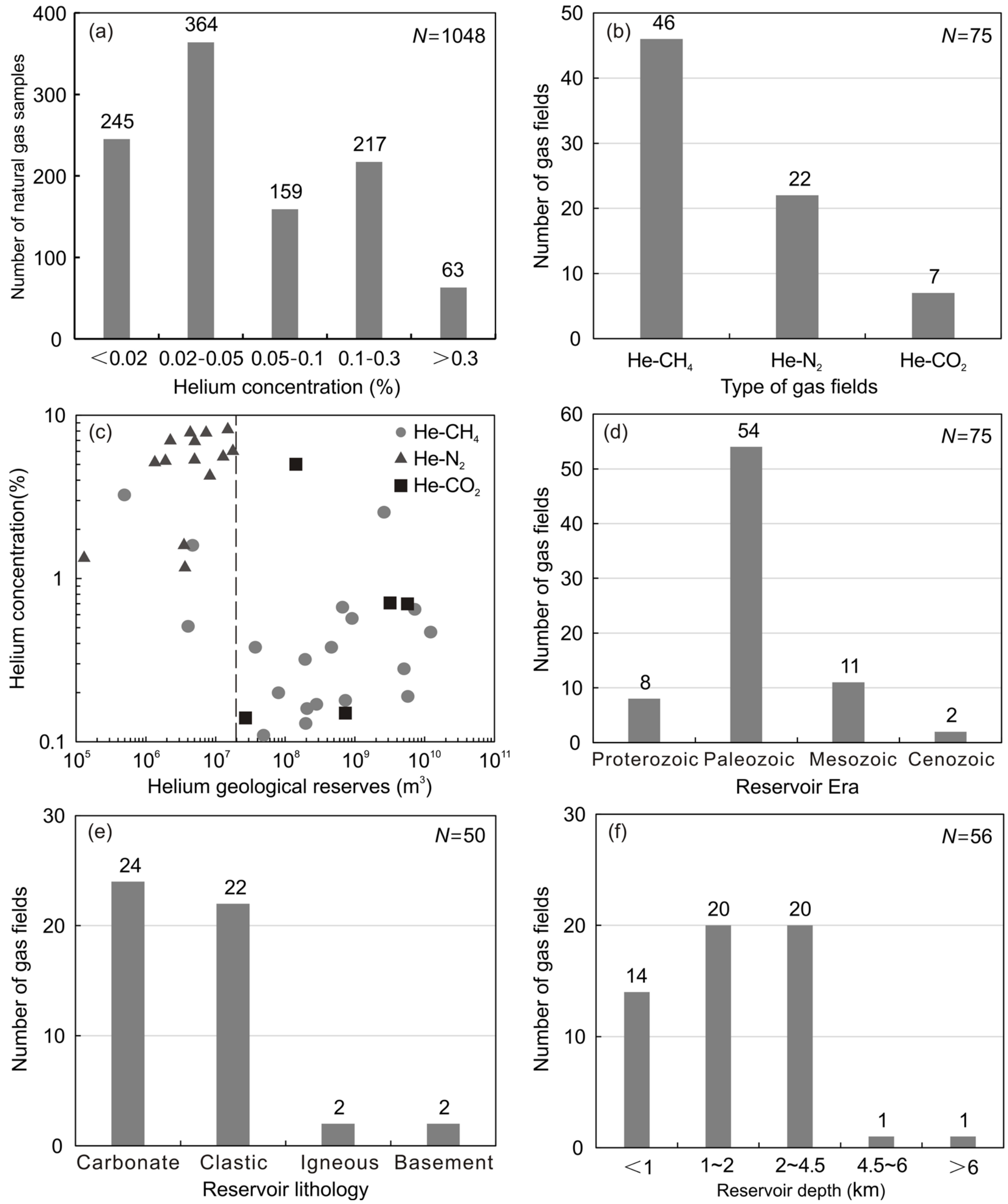

Figure 1 Geochemical characteristics of 75 helium-rich gas fields globally.

3.2 "Accompanying": Helium accumulates as a component accompanying other gases

To date, independent helium gas fields have not been found in nature. Helium, mainly in the form of trace component, accompanies natural gas components in He-CH_4, He-CO_2, He-N_2, and He-H_2 gas fields (Brown, 2010; Guélard et al., 2017). He-CH_4 gas fields are distributed in petroliferous basins in both ancient craton and tectonically active zones. However, He-CO_2 and He-N_2 gas fields are mainly distributed in petroliferous basins of tectonically active zones, such as those in eastern China, the Colorado Plateau in the United States and southeastern Australia (Xu et al., 1990; Xu, 1997; Liu K X et al., 2023; Tedesco, 2022). Among the 75 helium-rich gas fields worldwide (7 in China, 43 in the United States, 15 in Canada, 8 in Russia, 1 in Algeria, and 1 in Poland), there are 46 He-CH_4, 22 He-N_2, and 7 He-CO_2 gas fields, respectively, accounting for 61%, 29%, and 9% of the sampled gas fields, respectively (Figure 1b).

Helium geological reserves are estimated using the volumetric method. Helium geological reserves and helium concentrations in diverse types of helium-rich gas fields vary greatly. Specifically, $He-N_2$ gas fields typically have high helium concentrations (1–8%), but their geological reserves are often low, and discovered $He-N_2$ gas fields typically have helium geological reserves of less than 2×10^7 m^3 (Figure 1c). Additionally, both $He-CH_4$ and $He-CO_2$ gas fields generally have low helium concentrations, with the vast majority less than 1%, but their geological reserves are relatively high. For $He-CH_4$ gas fields, except for the Otis-Albert, Tocito Dome, and Tocito Dome North gas fields in the United States, which have reserves of less than $2\times10^7m^3$ (4.66×10^6 m^3, 4.04×10^6 m^3, and 0.49×10^6 m^3, respectively), the other 16 gas fields have helium reserves between 3.7×10^7 m^3 and 1.22×10^{10} m^3, with an average of 2.284×10^9 m^3 (Figure 1c). Five $He-CO_2$ gas fields (the Big Piney-La Barge, McCallum, Doe Canyon, McElmo Dome and St. John's Dome in the United States) have helium reserves between 2.7×10^7 m^3 and 5.663×10^9 m^3, averaging 1.946×10^9 m^3 (Figure 1c).

$He-CH_4$ gas fields are mainly distributed in ancient cratonic basins, where the scale of helium resources is generally large. Currently, $He-CH_4$ gas fields are the major type of gas field available for global helium extraction. The Hugoton-Panhandle gas field in the United States is located in the North American Craton, where the average helium concentration is 0.532%, and its helium geological reserves reach 1.22×10^{10} m^3. The Chayandinskoye and Kovyktinskoye gas fields in Russia are located in the Siberian Craton, where their average helium concentrations are 0.65% and 0.28%, respectively, and their helium geological reserves are 7.19×10^9 m^3 and 5.06×10^9 m^3, respectively. The Hassi R'Mel gas field in Algeria is located in the Sahara Craton, where the average helium concentration is 0.19%, and its geological helium reserves are 5.70×10^9 m^3. The Hetianhe and Dongsheng gas fields in China are located in the Tarim and Ordos Basins, respectively, their helium concentrations are 0.32% and 0.13%, respectively, and their helium geological reserves are 1.92×10^8 m^3 and 1.96×10^8 m^3, respectively

3.3 "Complex": Helium demonstrates complex spatial distribution patterns

Petroleum exploration activities have shown that helium generally accumulates with other accompanying components in different types of petroliferous basins, various strata with different geological ages, different types of reservoirs, and diverse burial depths (Yang et al., 1991; Xu et al., 1997a, 1998；Feng et al., 2001; Geerk et al., 2001; Wang et al., 2007; Zhang et al., 2008; Zenget al., 2013; Ni et al., 2014; Liu et al., 2015; Guo et al., 2016; Dai et al., 2017, Lyu and Jiang, 2017; Rafik and Kamel, 2017; Li Y H et al., 2018; Luo et al., 2019; Wang et al., 2020; Liu K X et al., 2022; Li J Y et al., 2022; Liu Q Y et al., 2022; Peng et al., 2022; Tedesco, 2022), which indicates the complex accumulation mechanisms of helium in the subsurface. Considering the helium-enriched strata, 54 helium-rich gas fields are located in the Paleozoic strata, accounting for 72%, while 8 and 11 helium-rich gas fields are in the Proterozoic and Mesozoic strata, respectively; only 2 helium-rich gas fields are in the Cenozoic strata (Xiqiao Gas Reservoir in China and Dineh-Bi-Keyah Field in the United States), both of which are $He-N_2$ gas fields (Figure 1d). From the perspective of reservoir lithology, carbonate and clastic rocks are major reservoir types, with 24 and 22 carbonate and clastic rocks, respectively (Figure 1e). Considering the depth, there are great differences among the diverse helium-rich gas fields, which are mainly shallower than 4500 m. The numbers of helium-rich gas fields at depths less than 1000 m, between 1000 m and 2000 m, and between 2000 m and 4500 m are 14, 20, and 20, respectively (Figure 1f). Ultimately, considering basin types, both cratonic basins and tectonically active zones have helium-rich gas fields with notable differences in $^3He/^4He$ ratios. The former has $^3He/^4He$ ratios in the range of 10^{-8}–10^{-7}, which are indicative of a typical crustal origin, while the latter has $^3He/^4He$ ratios in the range of 10^{-7}–10^{-6}, which are indicative of a crust-mantle mixing origin (Table 2).

Table 2 Isotope characteristics of helium in various types of petroliferous basins

Tectonic setting	Basin	$^3He/^4He$ ratio			References
		Range	Average	Number (N)	
Central and western cratonic basins	Tarim	1.4×10^{-8}–7.7×10^{-7}	8.0×10^{-8}	144	Xu et al. (1998); Chen et al. (2000); Liu et al. (2009, 2012, 2018); Yu et al. (2013); Dai et al. (2014); He et al. (2015, 2020); Tao et al. (2019)
	Qaidam	1.0×10^{-8}–6.8×10^{-8}	3.0×10^{-8}	10	Zhang et al (2020); Qin et al. (2022)

	Junggar	2.0×10^{-8}–5.4×10^{-7}	1.1×10^{-7}	33	Xu et al. (2017)
	Ordos	0.9×10^{-8}–1.4×10^{-7}	4.4×10^{-8}	105	Dai et al. (2017); Liu Q Y et al. (2022); Peng et al. (2022)
	Sichuan	$<0.1\times10^{-8}$–7.0×10^{-8}	2.0×10^{-8}	85	Ni et al. (2014); Qin et al. (2022)
Eastern tectonically active zones	Songliao	1.4×10^{-7}–8.2×10^{-6}	3.1×10^{-6}	87	Liu et al. (2014, 2016); Dai et al. (2017)
	Bohai Bay	1.5×10^{-8}–5.5×10^{-6}	1.8×10^{-6}	140	Zhang et al. (2008); Ni et al, (2022); Wang et al. (2022)
	Subei	6.0×10^{-7}–3.4×10^{-6}	3.4×10^{-6}	50	Xu et al. (1998); Liu Q Y et al. (2017); Wang et al. (2022)
	Sanshui	1.7×10^{-6}–6.4×10^{-6}	5.1×10^{-6}	9	
	Pearl River Mouth	1.6×10^{-6}–9.7×10^{-6}	4.9×10^{-6}	14	Wang et al. (2022)
	Yinggehai	4.9×10^{-8}–2.2×10^{-6}	3.7×10^{-7}	17	
	Qiongdongnan	6.0×10^{-6}–8.8×10^{-6}	7.1×10^{-6}	4	

4 Analysis of the key factors and mechanisms of helium accumulation

4.1 Identification of helium sources

4.1.1 Helium origins

Three separate sources of helium are found in natural gas: atmospheric, crust-derived, and mantle-derived helium (Xu et al., 1998; Dai et al., 2003). Atmospheric helium is released mainly through volcanic eruptions, magma degassing, and rock weathering (Ballentine and Burnard, 2002). Helium concentration in dry atmosphere is only 5 ppm, which is a result of dynamic balance processes between the Earth's degassing and the escape of helium into outer space (Ballentine and Burnard, 2002; Ozima and Podosek, 1983). Due to low concentration of atmospheric helium, the quantity of helium entering a basin geological system through sedimentation and groundwater circulation can usually be ignored. Crust-derived helium, mainly ^4He, is formed through the alpha decay of uranium (U) and thorium (Th) in rocks ($^{238}U\rightarrow8^4He+6\beta+^{206}Pb$, $T_{1/2}=4.468\times10^9$ years; $^{235}U\rightarrow7^4He+4\beta+^{207}Pb$, $T_{1/2}=7.1\times10^8$ years; $^{232}Th\rightarrow6^4He+4\beta+^{208}Pb$, $T_{1/2}=1.401\times10^{10}$ years) (Oxburgh et al., 1986; Ballentine and Burnard, 2002; Brown, 2010). Although the concentrations of U and Th in rocks are only on the order of 10^{-6}, and the helium production rate per unit volume per unit time by decay is also very insignificant, for example, per gram of U and Th per year produce only 1.21×10^{-7} cm^3 and 2.87×10^{-8} cm^3 of helium, respectively, helium still accumulates on a considerable scale in the crust over a long geological period due to the presence of large volumes of rocks (Ballentine and Burnard, 2002). Researchers generally believe that the annual production of ^4He via the decay of U and Th in the crust is approximately 8.0×10^6 m^3 (Porcelli and Ballentine, 2002). Mantle-derived helium is mainly considered primitive helium that occurs within the Earth's interior. This process has occurred since the formation of the Earth, where the ^3He concentration is significantly higher than that of crust-derived helium (Oxburgh et al., 1986).

Helium isotopic compositions from different sources also vary notably. In this regard, the helium isotopes ($^3He/^4He$ ratios) of mantle-derived helium, crust-derived helium, and atmospheric helium are $n\times10^{-5}$, $n\times10^{-8}$, and 1.4×10^{-6}, respectively. In general, 1.1×10^{-5} and 2×10^{-8} are regarded as the endmembers for mantle-derived helium and crust-derived helium, respectively (Lupton et al., 1983; Xu, 1997). According to the crust-mantle two-endmember mixing model (Xu et al., 1995), the contribution of mantle-derived helium to natural gas can be quantitatively evaluated. For instance, the $^3He/^4He$ ratios in natural gas from the Qingshen gas field in the Songliao Basin are 1.08×10^{-6}–8.18×10^{-6} (N=16), and the contributions of mantle-derived helium are estimated to be 9.4–72.9% (Liu et al., 2016). The $^3He/^4He$ ratios in natural gas from the Sacramento Basin in the United States are 1.5×10^{-7}–3.86×10^{-6} (N=20), and the contributions of mantle-derived helium are 1.2–35.2% (Poreda et al., 1986). The $^3He/^4He$ ratios in natural gas from the Niigata and Akita regions in Japan are $<1.4\times10^{-6}$–1.09×10^{-5} (N=13), and the contributions of mantle-derived helium are known to be <12.6–

99.1% (Sakata et al., 1986).

$$He_{Mantle}(\%)=[(^3He/^4He)_{Sample}-(^3He/^4He)_{Crust}]/[(^3He/^4He)_{Mantle}-(^3He/^4He)_{Crust}] \quad (1)$$

where He_{Mantle} (%) represents the contribution of mantle-derived helium, $(^3He/^4He)_{Mantle}$, $(^3He/^4He)_{Crust}$, and $(^3He/^4He)_{Sample}$ represent the helium isotopes of mantle-derived endmember, crust-derived endmember, and sample, respectively.

Helium isotopes in natural gas from petroliferous basins in China show significant regional variability (Xu, 1997). Tectonically, under the tectonic background of the subduction of the Western Pacific Plate, mantle-derived volatiles (containing abundant ^3He) migrate upwards along the deep-seated fault system and accumulate in the sedimentary strata. Therefore, the $^3He/^4He$ ratios in eastern tectonically active zones generally range from $n\times10^{-7}$ to $n\times10^{-6}$ (Table 2), with maximum contribution of mantle-derived helium reaching 88%. For cratonic basins in central and western China, due to the lack of a large amount of mantle-derived fluids in sedimentary basins, the $^3He/^4He$ ratios range from $n\times10^{-8}$ to $n\times10^{-7}$ (Table 2), which is mainly crust-derived helium, and the contribution of mantle-derived helium generally does not exceed 5%.

Although mantle-derived helium contributes to more than 90% of the total amount in some natural samples, no stand-alone mantle-derived helium gas field has been discovered in nature. Tectonically active zones are mainly crust-mantle complex helium resources, while cratonic basins are largely crust-derived helium resources. Although crust-mantle complex helium resources lead to industrial accumulation in petroliferous basins in Eastern China, this type of helium resource has not yet been commercially exploited due to the relatively small scale of natural gas resources and the strong heterogeneity in the helium concentration in natural gas. Crust-derived helium resources, such as the Hugoton-Panhandle gas field in the United States, the Hassi R'Mel gas field in Algeria, the North Par gas field in Qatar, and the Weiyuan and Dongsheng gas fields in China, are known to be the major type for industrial extraction worldwide.

4.1.2 Crust-derived helium

4.1.2.1 Types of helium source rocks

Unlike hydrocarbon source rocks, the types and geochemical evaluation of helium source rocks are still in their infancy, and the concentrations of U and Th in helium source rocks are currently receiving much attention. Granite is considered a very important helium source rock, which is consistent with the fact that large-scale ancient granite-metamorphic rocks have been discovered beneath helium-rich gas fields, such as the Hugoton-Panhandle and Dongping gas fields (Ballentine et al., 2002; Li Y H et al., 2018; Wang et al., 2020; Zhang et al., 2020). Basement rocks beneath these helium-rich gas fields have slightly higher concentrations of U and Th relative to those in the upper crust (Table 3).

Table 3 Concentrations of U and Th in basement rock in typical helium-rich gas fields

Gas fields	U concentration (ppm)	Th concentration (ppm)	Sources
Hugoton-Panhandle	2.8	10.7	Ballentine and Sherwood Lollar (2002)
Dongsheng	2.59	10.71	Wang et al. (2023)
Dongping	3.2	20.99	Liu Y T et al. (2023)
Upper crust	2.5	10.3	Hans Wedepohl (1995)

Concentrations of U and Th in both organic matter-rich shale and bauxite are significantly greater than those in the upper crust. For example, the concentration of U in theCambrian shale in the Sichuan Basin exceeds 40 ppm (Meng et al., 2021). Similarly, the concentration of U in the BG1 black shale from the Cambrian Yuertusi Formation in the northwestern margin of the Tarim Basin is as high as 52.98 ppm (Chen J F et al., 2023). Additionally, the concentrations of U and Th in the Carboniferous bauxite in the Ordos Basin are as high as 80.69–153.76 ppm (102.1 ppm on average) and 24.14–38.41 ppm (28.7 ppm on average), respectively (Liu D et al., 2022). Due to their high abundances of U and Th, both organic matter-rich shale and bauxite are also considered as important types of helium source rocks.

4.1.2.2 Distributions of U/Th-rich minerals

U/Th-rich minerals in helium source rocks are the main components in producing helium. Researchers used field emission scanning electron microscopy and electron probes to observe U/Th minerals in helium source rocks from different regions, where diverse types of U/Th minerals were discovered (Table 4). Such minerals mainly occur in quartz, feldspar, and biotite (Zhang, 2019; Liu, 2021; Meng et al., 2021; Zhang et al., 2022). Alpha particles that are released during the decay of U/Th minerals ionize their surrounding minerals, forming a radioactive halo (Liu, 2021). Zhang et al. (2022) conducted a study on the Huashan complex rock mass at the southern edge of the Weihe Basin and argued that there were particular differences in the type of U/Th minerals in the Indosinian and Yanshanian intrusive rocks. These two phases of intrusive rocks led to the development of zircon, titanite, and apatite. In addition, in the former thorite was also abundant, while in the latter brown epidote was present in high amounts. Although various types of U/Th-rich minerals have been discovered, there is still a lack of systematic research associated with the occurrence characteristics of U/Th-rich minerals in different types of helium source rocks, as well as the symbiotic relationships among such type of minerals.

Table 4 Distributions of U/Th-rich minerals in the helium source rocks

Helium source rocks	Observation methods	Uranium and thorium minerals	Sources
Granite in the northern margin of the Qinling Mountain	Electronic probe	Betafite, thorite, uranothorite, uraninite, xenotime, monazite, zircon, apatite, allanite, titanite, rutile, bastnaesite, samarskite	Zhang (2019)
Granite, shale and sandstone in the upper Yangtze Platform	Field emission scanning electron microscope	Zircon, monazite, uranothorite, apatite, titanite, xenotime, etc.	Meng et al. (2021)
Granite in the northern margin of the Qinling Mountain	-	Uraninite, allanite, zircon, epidote, xenotime, titanite, magnetite	Liu (2021)
Granite in the southern margin of the Weihe Basin	Electronic probe	Zircon, titanite, apatite, allanite, thorite	Zhang et al. (2022)

Note: "-" represents no report.

4.1.2.3 Identification of helium sources in crust-derived helium gas fields

Almost all helium-rich gas fields have high nitrogen concentrations. N_2 sources in natural gas are complex and include mantle degassing, thermal maturity of organic matter, denitrification of organic sediment at overmatured stage, amino-rich clay, and low-temperature metamorphism (Halford et al., 2022). Considering the helium isotope characteristics of gases from the Canadian Shield, Hugoton-Panhandle gas field, Dongping gas field, Hetianhe gas field, Weiyuan gas field, and Dongsheng gas field (Sherwood Lollar et al.,1993, 2008; Ballentine and Sherwood Lollar, 2002; Ni et al., 2014; Tao et al., 2019; Peng et al., 2022; Liu Y T et al., 2023), it is inferred that these gas fields have no strong mantle-derived fluid activity, thus, the contribution of mantle degassing can be eliminated.

Natural gas reservoir in the Canadian Shield has a Precambrian volcanic-metamorphic basement. Because the carbon isotopes of alkanes show partial inversion, Sherwood Lollar et al. (1993, 2008) suggested that alkane gases are of inorganic origin. For this reason, it is inferred that N_2 may have originated from either amino-rich clay or low-temperature metamorphism. In the diagram of ($\sum C_{2+}/\sum C_{1+}$) versus $\delta^{13}CH_4$, except for four natural gas samples from the Dongping gas field, other natural gas samples from the Hugoton-Panhandle, Hetianhe, Weiyuan, Dongsheng, and Dongping gas fields do not plot in the overmatured thermogenic dry/wet gas zones (Figure 2a). This is because, prior to entering over-matured stage, organic matter generates only a small amount of N_2, which is consistent with the fact that N_2 concentration in most natural gas samples is below 2% (i.e., Zhang et al, 2008; Ni et al., 2014; Liu et al., 2015, 2018; Liu Q Y et al., 2022). However, except for those in the Dongsheng gas field, N_2 concentrations in the other helium-rich gas fields are significantly higher than 2% (Table 5). Thus, besides the organic matter, N_2 might have other sources, possibly the ancient basement.

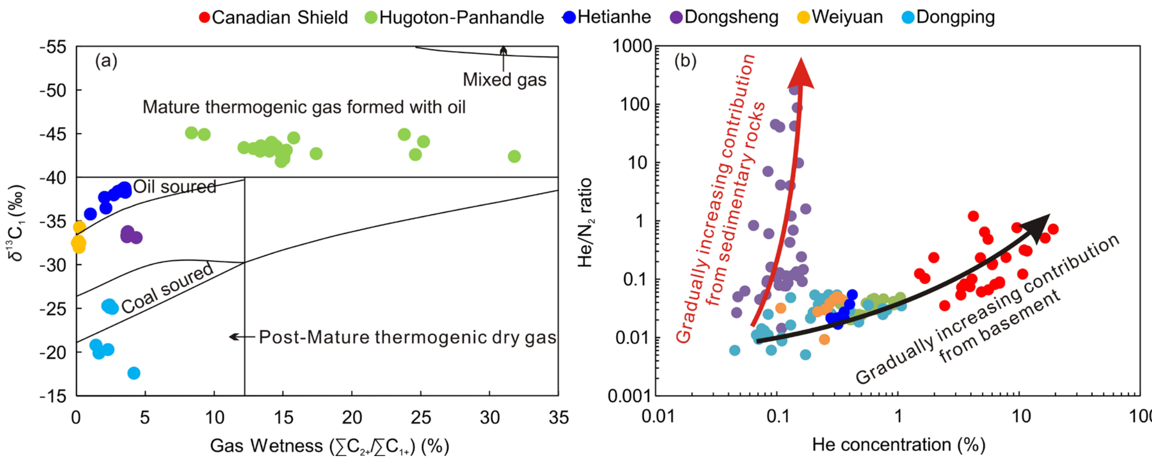

Figure 2 Diagram for identifying the sources of crust-derived helium. (a) Diagram of natural gas wetness ($\sum C_{2+}/\sum C_{1+}$) versus $\delta^{13}CH_4$ (after Halford et al., 2022); (b) diagram of He concentration versus He/N_2 ratio.

When He concentration is plotted against He/N_2 ratio, two distinct evolutionary pathways are observed (Figure 2b). In the Canadian Shield, Hugoton Panhandle gas field, Dongping gas field, Hetianhe gas field, and Weiyuan gas field, He concentration is positively correlated with He/N_2 ratio. Basement-rock helium gas field (Canadian Shield) has the highest He/N_2 ratio, mostly greater than 0.05, and has the greatest He concentrations, with all values greater than 1%. In the other four helium-rich hydrocarbon gas fields (Hugoton-Panhandle, Dongping, Hetianhe and Weiyuan gas fields), He/N_2 ratios are mostly less than 0.05, and He concentrations are almost all less than 1%. Although organic matter-rich shale contains high concentrations of U and Th with strong helium-generating potential, due to dilution from a large amount of hydrocarbon gases, it would be difficult to form helium-rich hydrocarbon gas fields that can be considered commercially valuable without an external helium supply. For example, helium concentration in Longmaxi shale gas in the Sichuan Basin is generally less than 0.04% (Nie et al., 2023). Moreover, there are certain differences in He/N_2 ratio and He concentration among the Hugoton Panhandle, Dongping, Hetianhe, and Weiyuan gas fields, which are attributed to differences in the contributions of basement rocks to the helium that is formed. As He/N_2 ratio decreases, the contribution of basement rocks to helium formation decreases, thus He concentration in hydrocarbon gas fields decreases as well.

However, for the Dongsheng gas field, there is no significant correlation between He concentration and He/N_2 ratio. Authors believe that contribution of basement rocks to helium in this helium-rich gas field is limited and that helium mainly originates from sedimentary rocks. He/N_2 ratios span a large range, up to 5 orders of magnitude and between 10^{-2} and 10^{3}. As hydrocarbon generation process ceased, organic matter-rich shale no longer generated hydrocarbon gases and N_2, while ongoing helium generation caused a steady increase in He/N_2 ratio. However, due to the long half-life and low helium production rate of U and Th, helium generation continues, and this did not cause a significant increase in helium concentration in this type of gas field.

In summary, given the geological background and geochemical characteristics of different types of crust-derived helium gas fields, in this study, three helium supply models are proposes. They include the following: basement, combined basement-sedimentary rock, and sedimentary rock helium supply types. The Canadian Shield exemplifies the basement helium supply type, characterized by natural gas containing very high concentrations of He and N_2. The Hugoton-Panhandle, Dongping, Hetianhe, and Weiyuan gas fields represent the combined basement-sedimentary rock helium supply type, where natural gas exhibits a relatively high N_2 concentration, but is notably lower than that of the basement helium supply type. In contrast, the Dongsheng gas field exemplifies the sedimentary rock helium supply type, where natural gas features a very low N_2 concentration.

Table 5 Distributions of N_2 and He concentrations in typical crust-derived helium-rich gas fields

Types	Gas fields	N_2 concentration (%)	He concentration (%)	Sources

Basement helium supply type	Canadian Shield	3.48–87.00/36.59	1.51–19.10/6.46	Sherwood Lollar et al. (1993, 2008)
Combined basement-sedimentary rock helium supply type	Hugoton-Panhandle	6.6–25.8/16.76	0.29–1.05/0.53	Ballentine et al. (2002)
	Weiyuan	3.09–26.70/8.26	0.003–0.342/0.24	Ni et al. (2014)
	Hetianhe	7.72–18.83/14.21	0.28–0.42/0.34	In this work
	Dongping	2.69–34.10/11.00	0.045–1.069/0.27	Zhang et al. (2020)
Sedimentary rock helium supply type	Dongsheng	0–7.61/0.70	0–0.39/0.14	Peng et al. (2022)

4.2 Primary migration

4.2.1 Migration patterns

Primary migration of helium refers to the process in which helium that is generated via radioactive decay of U and Th diffuses from the mineral lattice, intergranular or inclusions into pores. After the formation of minerals, most radiogenic ^{4}He remains within the mineral lattice, and is generally released from minerals through diffusion (Figure 3a), recoil (Figure 3b), fracturing (Figure 3c), and mineral transformation (Figure 3d) (Ballentine and Burnard, 2002).

Diffusion is an important process for the primary migration of helium at the mineral scale. Helium diffusion coefficient in fine-grained (0.1 mm) minerals in the upper crust (<150 °C) is 10^{-18}–10^{-22} cm/s (Lippolt and Weigel, 1988; Trull et al., 1991). With either the increase of the temperature or the decrease of diffusion domain size, helium diffusion coefficient shows an increasing trend. In addition, the morphology of the crystal particles can also affect helium diffusion (Ballentine and Burnard, 2002).

Recoil refers to the process in which high-energy α-particles that are produced by the decay of U and Th are ejected at a certain distance away from the parent nucleus, resulting in an α-damage track. Recoil distance of α-particles is on the same scale as grain size in fine-grained crustal rocks. Density of U and Th minerals, crystal grain size, and positions of parent U and Th all affect the position of daughter helium. In comparison to dry rocks, water-filled rocks result in an increase in the fraction of daughter helium that may be retained within mineral lattices (Ballentine and Burnard, 2002).

Dilatant fracturing refers to the inelastic failure of brittle rocks that occurs during compressional loading, which results from microfracturing prior to macroscopic fracturing. Lattice fracturing leads to the rapid release of helium trapped within mineral lattices into pore spaces. Torgersen and O'Donnell (1991) conducted a numerical study to examine the effect of rock fracturing on helium release using a one-dimensional slab of infinite length. Their results showed that the gas flux released out of the rock increases as a function of the fracture spacing of the slabs.

Mineral transformation also leads to the release of helium trapped within mineral lattices. Common mineral transformation processes include diagenesis (e.g., illite→montmorillonite), metamorphism (e.g., recrystallization of clay minerals to biotites, amphiboles), and mineral alteration (e.g., serpentinization of mafic minerals). Because helium is an incompatible element, helium that is generally released during mineral transformation is less likely to be found in new mineral phases (Ballentine and Burnard, 2002).

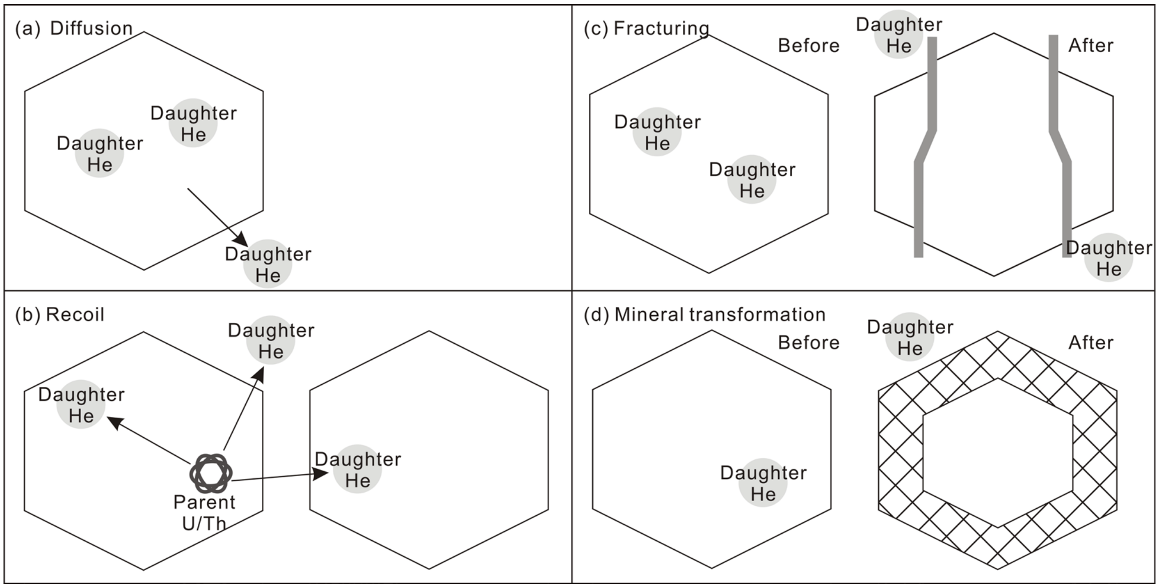

Figure 3 Schematic diagram of helium primary migration (after Ballentine and Burnard, 2002). (a) Diffusion; (b) recoil; (c) fracturing; (d) mineral transformation.

4.2.2 ^{4}He closure temperature

Helium diffusion in minerals is mainly constrained by temperature. Dodson (1973) proposed the ^{4}He closure temperature based on activation energy diffusion process of helium in rock masses, as shown in formula (2). When temperature is above the ^{4}He closure temperature of certain minerals, helium produced by the decay of U and Th is released from mineral lattices. Moreover, as temperature increases, the diffusion ability of helium tends to increase significantly, while the time for helium that is released from mineral lattices shortens sharply. For example, at temperatures less than 40 °C, all helium is retained within the mineral lattice of apatite. Once temperature exceeds 90 °C, helium is released from mineral lattices for an extended period. At temperatures between 40°C and 90°C, helium is partially released through diffusion (Wolf, 1998).

$$T_c = \frac{E_a / \mathrm{R}}{\ln\left[\left(ART_c^2 D_0 / r^2\right) / \left(E_a dT / dt\right)\right]} \qquad (2)$$

where T_c is closure temperature, D_0 is diffusion coefficient at infinite temperature, E_a is activating energy, r is radius of grain, R is gas constant, 8.314J/(mol·K), A is a constant characterizing the shape of grain, A=55, 27, and 8.7 for sphere, cylinder, and slab, respectively, and dT/dt is cooling rate.

Differences in ^{4}He closure temperatures among diverse U/Th-rich minerals vary greatly. ^{4}He closure temperatures of both uraninite and apatite are commonly less than 100°C, while for betafite, zircon, titanite, hematite, magnetite, and monazite they are between 100°C and 300°C, and for garnet it can be as high as 590-630 °C (Bähr et al., 1994; Lippolt et al., 1994, Dunai and Roselieb, 1996; Wolf et al., 1996; Reiners and Farley, 1999; Farley, 2000, 2002; Boyce et al., 2005; Reiners, 2005; Shusteret al., 2006; Reichet al., 2007; Cherniak et al., 2009; Zhang, 2019). Given that helium source rocks typically contain various U and Th minerals (Zhang, 2019; Meng et al., 2019; Liu, 2021; Zhang et al., 2022), and that a wide range of ^{4}He closure temperatures associated with these rocks, the release of helium becomes more complicated. This complexity poses challenges for accurately evaluating the helium flux emitted from helium source rocks.

4.3 Helium exsolution

Amount of helium dissolved in formation water follows Henry's law, as shown in formula (3), which was proposed by Henry in 1803. This law states that under certain temperature conditions, gas solubility in formation water is a function of equilibrium partial pressure, (Brown, 2010).

$$\boldsymbol{P_B = K_{x,B} \times x_B} \qquad (3)$$

where P_B is the partial pressure of certain gases at equilibrium, $K_{x,B}$ is Henry's constant, and x_B is the mole fraction of certain gases dissolved in solution.

Temperature affects the solubility of helium in formation water (Pray et al.,1952; Wilhelmet al., 1977; Potter and Clynne, 1978; Crovetto et al., 1982; Fu et al., 1996； Brown, 2010; Abrosimov and Lebedeva, 2013). As temperature gradually decreases, Henry’s constant gradually increase (Figure 4a). This implies that from deep to shallow depths, the solubility of helium in formation water gradually decreases; that is, the occurrence of helium decrease from the dissolved to free state. At the same depth, the formation water samples with a high geothermal gradient have low gas to water ratio of helium (Figure 4b), which is due to more helium dissolving in the formation water.

There are significant differences in the solubilities of different gases in formation water under different temperature conditions (Figure 4b). At diagenetic temperature, Henry's constant of helium is significantly higher than that of nitrogen and methane (at the same partial pressure), indicating that helium has the lowest solubility. At metamorphic temperature, Henry's constant of nitrogen is the highest, and Henry's constants of helium and methane tend to be the same, indicating that nitrogen has the lowest solubility. Temperature and pressure levels used in gas dissolution/exsolution experiments with formation water are relatively low. Thus, there are limited data available on the dissolution/exsolution of multicomponent systems (such as He-N_2-CH_4) under high-temperature and high-pressure conditions resembling those found in deep formations, and further studies are needed.

As the salinity of formation water increases, Henry's coefficient increases sharply (Figure 4a), indicating a severe decrease in helium solubility in high-salinity formation water (Brown, 2010). Formation water in the Shenguhao, Duguijiahan, and Shilijiahan blocks on the eastern edge of the Paerjianghaizi Fault in the Dongsheng gas field is the $CaCl_2$ type, with total salinities of 16.8-61.4g/L (Zhao et al., 2022). Statistical results show that for these three blocks, helium concentrations are approxiamtely negatively correlated with the salinity of formation water (Figure 4c), possibly due to the low solubility of helium in high-salinity formation water. In addition, there are various types of formation water according to the Sulin classification, such as $MgCl_2$, $CaCl_2$, Na_2SO_4, and $NaHCO_3$, while the differences in helium solubility in different types of formation water are rarely reported.

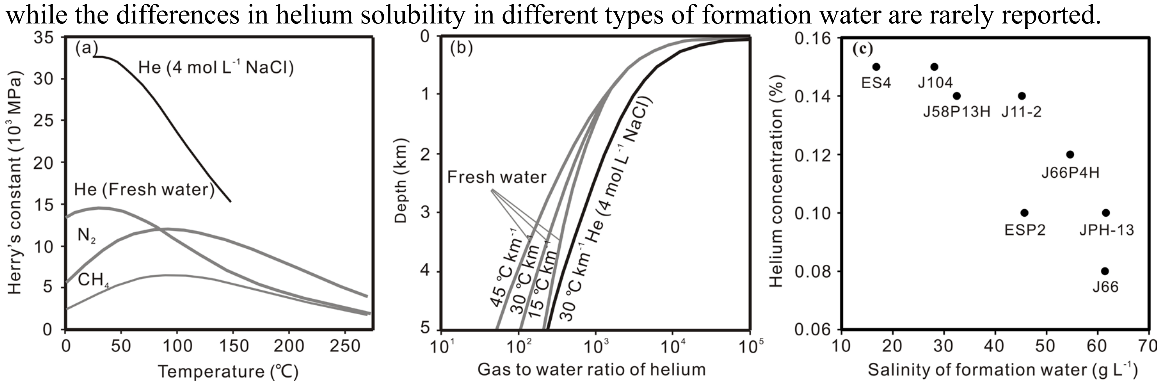

Figure 4 Factors influending the solubility of helium in formation water. (a) Relationship between Henry’s constant of helium and temperature; (b) relationship between gas to water ratio of helium and depth; (c) relationship between helium concentration and the salinity of formation water in the Dongsheng gas field. Figures 4a and 4b are modified based on Brown (2010), and the data associated with helium concentrations and the salinity of formation water within Figure 4c are from Peng et al. (2022) and Zhao et al. (2022), respectively.

A sharp change in the partial pressure of helium is an important mechanism for helium exsolution from formation water (Brown, 2010; Sathaye et al., 2016; Li et al., 2017; Cheng et al., 2023). Most helium-rich gas fields that are found in the basement as well as in the upper part of ancient cratonic basins have high N_2 concentrations, where both N_2 and He may have originated from ancient basement granite-metamorphic rocks. Using a combination of field data analysis (from the Williston Basin) and numerical simulation, Cheng et al. (2023) demonstrated the process of helium exsolution in initial He-N_2-rich fluids. When the dissolved N_2 in formation water reaches saturation, it separates into a distinct gas-phase. During this process, N_2 “effectively strips” helium from the dissolved state in the formation water, creating a unique He-N_2 temporary “repository”, which eventually migrates to favorable traps for enrichment (Cheng et al., 2023). If N_2 dissolved in the formation water does not reach full saturation, He and N_2 typically comigrate in the dissolved state with the formation water. When helium-containing formation water encounters gaseous hydrocarbons, the partial pressure of helium significantly decreases, resulting in helium exsolution alongside the gaseous hydrocarbons. In the case where helium-containing formation water mixes with liquid hydrocarbons, helium is redistributed between two geological fluids due to differences in helium solubility.

In addition, competitive dissolution of different types of gases may also be an important mechanism for helium enrichment. A prerequisites for proposing this mechanism of helium enrichment is that gas-phase dissolution sites in formation water are constant. If gas-phase dissolution sites in formation water approach saturation, helium exsolution means that other gaseous components occupy the original dissolution sites of helium in formation water. In summary, further research is needed to determine which enrichment mechanism predominates or if there are additional mechanisms involved.

4.4 Secondary migration

Helium secondary migration refers to the process in which following primary migration, helium migrates and accumulates in favorable traps. This is a very complex process, during which deep-seated faults are considered important pathways for secondary migration of helium-containing fluids. In addition to crust-derived same-source helium gas fields, secondary migration of helium must occur via a carrier. There are various types of helium-containing fluids, including helium-hydrocarbon (gaseous and liquid) mixtures, He-nonhydrocarbon (mainly CO_2, N_2 and H_2) mixtures, helium-containing formation water, and helium-containing mantle-derived fluids. Types of helium-containing fluids are a function of multiple factors, such as the source of helium as well as its fluxes, accompanying components as well as their fluxes, properties and scales of geological fluids, and interactions between helium-containing fluids and hydrocarbon fluids.

Although helium can migrate through diffusion, authors suggest that migration distance in this process is very limited. On a geological timescale, helium concentrations in natural gas, especially coalbed methane and shale gas, in petroliferous basins exhibit strong horizontal and vertical heterogeneity, indicating that diffusion is not the major reason for the secondary migration of helium.

Formation and evolution of fault systems control the structural framework of basins, the migration pathways of oil and gas accumulations, and the development and evolution of traps (Liu Y H et al., 2017; Wang et al., 2017; Li S Z et al., 2018; Zhu and Xu, 2019). Overall, for either crust-derived helium gas fields in ancient cratonic basins or crust-mantle complex helium gas fields in tectonically active zones, assuming that deep-seated faults do not damage the sealing of the traps, it is generally known that closer proximity to the fault zone should cause a more pronounced anomalous helium patterns in gas fields.

Two sets of nearly vertically intersecting deep-seated faults have developed in the northern part of the Songliao Basin. Zones with high helium concentrations are mainly found in deep-seated faults as well as their peripheries, especially at the intersection of two crustal faults, F4 (Renminzhen-Zhaozhou Fault Zone) and F6 (Binzhou Fault Zone). Helium concentration in natural gas from Well Wang 9-12, which is located in the northern part of the Sanzhao Depression, is as high as 2.104% (Figure 5) (Feng et al., 2001; Zhong, 2017). Liaohe Basin includes Eastern Depression and Western Depression, which are parallel to the fault direction. Eastern Depression is located in the major fault zones and their western edge, while the Western Depression is separated by a protrusion and is not connected to deep-seated fault zones. Therefore, helium concentrations in the Eastern Depression are 32–988 ppm, with an average of 176 ppm, which is significantly higher than that in the Western Depression (7–64 ppm, 30 ppm on average). The measured $^3He/^4He$ ratios in the Eastern Depression are in the range of 0.155×10^{-6}–5.46×10^{-6}, with an average of 2.55×10^{-6}; whereas those in the Western Depression are significantly lower, with a magnitude of 10^{-7} (Xu et al., 1998).

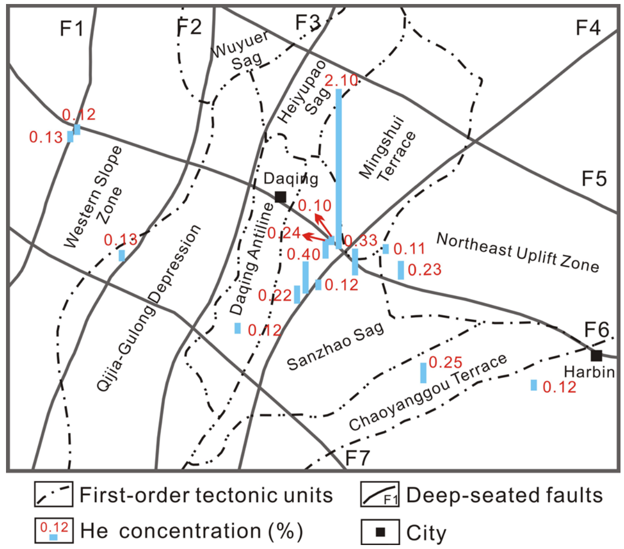

Figure 5 Distributions of deep-seated faults and helium concentrations in northern Songliao Basin (after Zhong (2017).

4.5 Tracing of helium-including fluids

Noble gases (He, Ne, Ar, Kr, and Xe) are not easily affected by changes in biological and chemical conditions. Therefore, the isotopic compositions of noble gases are ideal tracers for studying the interactions of underground fluids (mixing, dissolution/exsolution, diffusion) (Ballentine and Burnard, 2002, Li Y et al., 2022). Some noble gas components (i.e., ^{20}Ne, ^{36}Ar, ^{84}Kr, and ^{130}Xe) are mainly from the atmosphere, and they enter underground fluid system through the recharging of surface water. When formation water meets hydrocarbon fluids, noble gas components undergo fractionation due to differences in solubility (Figure 6). Based on the geochemical characteristics of noble gases in geological fluids, the interactions between hydrocarbon fluids and formation water can be quantitatively evaluated, thereby enabling the tracking of helium migration and accumulation processes.

At temperature less than 77 °C, the solubility of noble gases in water is positively proportional to their relative molecular weight, that is, Xe>Kr>Ar>Ne (Crovetto et al., 1982). Due to the higher solubility of noble gases in the oil phase, noble gas components in water phase preferentially transfer to the oil phase when two-phase fluids mix, resulting in a decrease in the concentrations of noble gases in the water phase. Ar has a higher solubility in the oil phase and tends to transfer to the oil phase relative to Ne. Therefore, after oil-water fractionation equilibrium, the oil phase should have a lower $^{20}Ne/^{36}Ar$ ratio, whereas the water phase should have a high $^{20}Ne/^{36}Ar$ ratio. When water and gas phases meet, Ne tends to transfer to gas phase relative to Ar. Therefore, after gas-water fractionation equilibrium is reached, the $^{20}Ne/^{36}Ar$ ratio in the gas phase become higher, whereas in the water phase, it decrease (Battani et al., 2000).

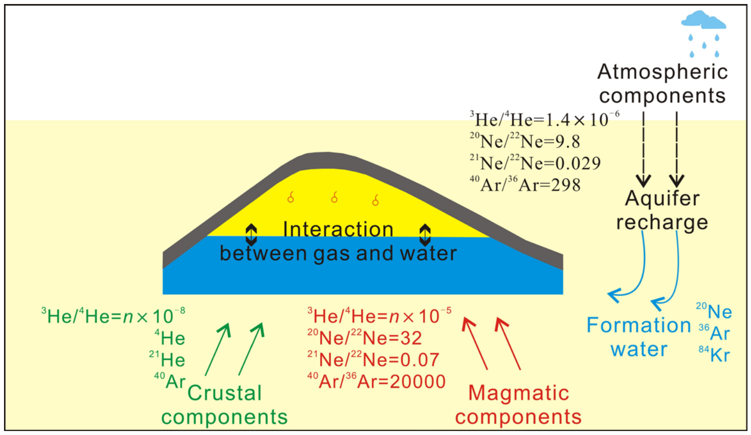

Figure 6 Schematic diagram of noble gas isotopes from different sources in a petroleum system.

Regarding the fractionation processes of noble gases during interactions between formation water and oil/gas phase, researchers have proposed two fractionation modes: batch fractionation in closed systems and Rayleigh fractionation in open systems. These two fractionation modes are represented by formulas (4) and (5), respectively (Ballentine et al., 2002). According to the diagram of noble gas isotope ratios, i.e., the diagrams of $^{84}Kr/^{36}Ar$ ratio versus $^{20}Ne/^{36}Ar$ ratio, as well as $^{130}Xe/^{36}Ar$ ratio versus $^{20}Ne/^{36}Ar$ ratio, the sealing of oil-water and gas-water fractionation systems can be distinguished.

$$\left(\frac{A}{B}\right)_{\text{water}}=\left(\frac{A}{B}\right)_{\text{ASW}}\times\left(\frac{V_{\text{water}}\rho_{\text{water}}}{V_{\text{oil}}\rho_{\text{oil}}}+\frac{(K_B)_{\text{water}}}{(K_B)_{\text{oil}}}\middle/\frac{V_{\text{water}}\rho_{\text{water}}}{V_{\text{oil}}\rho_{\text{oil}}}+\frac{(K_A)_{\text{water}}}{(K_A)_{\text{oil}}}\right) \tag{4}$$

where $\left(\frac{A}{B}\right)_{\text{water}}$ and $\left(\frac{A}{B}\right)_{\text{ASW}}$ are the ratio of noble gas A and B in formation water after oil-water fractionation and in air-saturated formation water, respectively, V_{water} and V_{oil} are the volume of water and oil phases, respectively, ρ_{water} and ρ_{oil} are the density of water and oil phases, respectively, $(K_A)_{\text{water}}$ and $(K_A)_{\text{oil}}$ are the Henry's constant of noble gas A in water and oil phases, respectively, and $(K_B)_{\text{Water}}$ and $(K_B)_{\text{Oil}}$ are the Henry's constant of noble gas B in water and oil phases, respectively.

$$\left(\frac{A}{B}\right)_{\text{water}}=\left(\frac{A}{B}\right)_{\text{ASW}}f^{\alpha-1} \tag{5}$$

Where f is the ratio of noble gas B retained in water phase after oil-water fractionation equilibrium, and α is fractionation coefficient.

In the Rayleigh fractionation, both dissolution and diffusion may control fractionation processes, while the α of gas-water fractionation process is controlled by dissolution and can be represented using Formula (6). Additionally, the α of oil-water fractionation process controlled by diffusion is defined using Formula (7), and the α of fractionation process controlled by diffusion can be explained by Formula (8) (Ballentine et al., 2002)

$$\alpha=(K_A)_{\text{water}}/(K_B)_{\text{oil}} \tag{6}$$

where $(K_A)_{\text{water}}$ are the Henry's constants of noble gas A in water.

$$\alpha=\left(\frac{(K_A)_{\text{water}}}{(K_B)_{\text{water}}}\middle/\frac{(K_A)_{\text{oil}}}{(K_B)_{\text{oil}}}\right) \tag{7}$$

$$\alpha=\sqrt{\frac{M_B}{M_A}} \tag{8}$$

where M_A and M_B are the molecular weights of noble gas A and B, respectively.

Based on the noble gas isotope fractionation theory, some scholars have comprehensively discussed helium migration and accumulation processes in the Hugoton-Panhandle gas field, Four Corners region and San Juan Basin in the United States, as well as the Weihe Basin and the northern region of the Qaidam Basin in China (Ballentine and Sherwood Lollar, 2002; Zhou et al., 2005; Gilfillan et al., 2008; Danabalan, 2017; Zhang et al., 2019a, 2019b; Halford et al., 2022).

4.6 Helium accumulation and preservation

Helium-rich gas fields worldwide are mainly distributed in cratonic basins and their peripheries under the background of the late Proterozoic-Paleozoic platform (Yakutseni,2014). Moreover, since the Mesozoic-Cenozoic deep structures have undergone relatively strong tectonic movements or magmatic activity, during which fault systems formed, such settings create important pathways for helium migration (Kennedy and van Soest, 2006). On the other hand, heat carried by magma activity "bakes" rocks, which favors the rapid release of helium (Hand,2016).

Tectonically, commercially minable helium-rich gas fields are mainly distributed in the (ancient) uplifts of ancient cratonic basins as well as their peripheries. Hugoton-Panhandle gas field in the United States is located in the Amarillo-Wichito Uplift of the North American Craton, and the Weiyuan gas field is in the Leshan-Longnvsi ancient uplift on the southwest edge of the Upper Yangtze Plate. Three reasons can explain why uplifted areas are suitable for helium accumulation: (1) tectonic uplift leads to the formation of effective migration pathways in source-reservoir systems, (2) stratigraphic uplift causes significant decrease in reservoir pressure, favoring helium exsolution, and (3) uplifted areas have a weak dilution effect of hydrocarbon gases.

Sealing capacity of caprocks is vital for helium preservation. Helium has a dynamic diameter of only 0.26 nm, which is significantly smaller than those of CH_4, CO_2, and N_2 (0.38 nm, 0.33 nm, and 0.364 nm, respectively), and it strongly diffuses. In addition, helium has a very low generation rate, and effective accumulation of helium requires that the amount of loss must be lower than that of the supply for a gas reservoir to form. Therefore, the sealing properties of caprocks in helium-rich gas fields have become even more important. Caprocks in some helium-rich gas fields worldwide are evaporite and thick shale with strong sealing capacity (Table 6). Evaporite has a stronger sealing capacity than shale. Therefore, gas fields with evaporite as caprock commonly have higher helium concentrations.

Table 6 Characteristics of reservoirs and caprocks in the helium-rich gas fields worldwide

Helium-rich gas fields	Average helium concentration	Caprocks	Sources
Hetianhe gas field in the Tarim Basin in China	0.34%	Carboniferous Bachu and Kalashayi Formation mudstone	Zhou et al. (2006)
Dongsheng gas field in the Ordos Basin in China	0.13%	Permian Shihezi and Shiqianfeng Formation mudstone	He F Q et al. (2022); Peng et al. (2022)
Weiyuan gas field in the Sichuan Basin in China	0.26%	Cambrian dark mudstone	Liu (1992); Liu et al. (2008); Liu K X et al. (2022)
Hugoton-Panhandle gas field in the United States	0.53%	Permian Wichita Formation gypsum	Tedesco (2022)
Cliffside gas field in the United States	1.8%	Permian Panhandle Formation gypsum	Tade (1967); Li Y H et al. (2018)
Doe Canyon gas field in the United States	5.01%	Pennsylvania Paradox Formation salt and gypsum	Gilfillan et al. (2008)
Big Piney-La Barge regions in the United States	0.5%	Mississippi Madison Formation salt and evaporite	Becker and Lynds (2012)

Helium loss via diffusion is one of the major ways to destroy helium gas fields. Diffusion coefficient is a widely used parameter for quantitatively characterizing gas diffusion capacity (Li P P et al., 2018, Sun et al., 2023). Currently, commercially minable helium-rich gas fields are mainly He-CH_4 type, therefore, the helium diffusion coefficient (T=323.15 K, P=20 MPa) is calculated for diverse He-CH_4 mixture systems in this work, as shown in Figure 7. Helium diffusion coefficient is expressed using formulas (9), (10), and (11) (Civan, 2010; Wu et al., 2017; Sun et al., 2023). Helium diffusion coefficient increases with increasing helium concentration, indicating that without considering the sealing capacity of caprock, the higher the helium concentration is in helium-containing natural gas, the greater the flux of helium loss in the form of diffusion.

$$D_{\mathrm{He}}=\frac{v_{\mathrm{He}}\lambda_{\mathrm{He}}}{3} \tag{9}$$

$$v_{\mathrm{He}}=\sqrt{\frac{8RT}{\pi M_{\mathrm{He}}}} \tag{10}$$

$$\lambda_{\mathrm{He}}=\frac{4K_BT}{\pi P\sum_{j=1}^{2}n_j\left(\delta_{\mathrm{He}}+\delta_j\right)^2\sqrt{\left(1+M_{\mathrm{He}}/M_j\right)}} \tag{11}$$

where D_{He} is diffusion coefficient, in m^2/s,v_{He} is thermal average velocity, in m/s, λ_{He} is molecular mean free path, in m, R is gas constant, which is 8.314J/(mol·K), T is thermodynamic temperature, in K, M is molecular molar mass, in g/mol, Z is gas compressibility factor,K_B is Boltzmann constant, which is 1.3806×10^{-23}J/K, P is gas pressure, Pa, δ_{He} is the molecular dynamics diameter of helium, which is 0.26×10^{-9} m, j is the type of gas components in mixed system, δ_j is the molecular dynamics diameter of the j-th gas component in mixed system, in m, n_j is the concentration of the j-th gas component, in %.

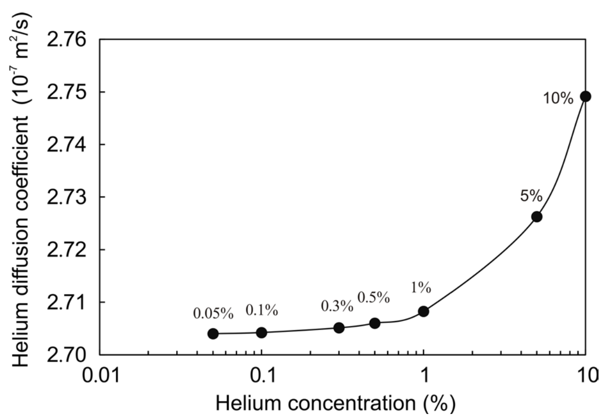

Figure 7 Helium diffusion coefficient in diverse mixed He-CH_4 systems.

4.7 Helium accumulation

Both helium and hydrocarbon gas accumulation systems depend on six essential factors: “generation, reservoir, caprock, trap, migration, and preservation”. They exhibit common characteristics, including from source rocks to traps for accumulation, which is a unique scenario for the occurrence of helium in geological bodies. However, the origins of helium and hydrocarbons are completely different, while migration-enrichment systems and accumulation conditions are similar.

Generation of hydrocarbons is mainly controlled by the abundance of organic matter, as well as its thermal maturity. Generation of crust-derived helium is mainly related to the concentrations of U and Th in helium source rocks, as well as decay time. Flux of mantle-derived helium is closely related to the scale of mantle-derived fluids, as well as activity periods.

For crust-derived same-source helium gas pools, both helium and hydrocarbon gases undergo in-situ or near-source accumulation. However, there are significant differences in the mechanisms of their primary migrations, but their secondary migrations are somewhat similar. Primary migration of helium is mainly controlled by formation temperature. Once ^{4}He closure temperature is exceeded, helium is released continuously. However, the primary migration of hydrocarbons is driven by hydrocarbon-generating pressurization, with a pattern of episodic expulsion.

In addition to in-situ or near-source accumulation, there are significant differences in migration and accumulation systems for both helium and hydrocarbons. Under thermal stress, hydrocarbon source rocks generate large amounts of hydrocarbons in a short period (compared to the half-life of helium source rocks). Driven by fluid pressure and buoyancy, these hydrocarbons, in the form of continuous fluids, migrate into favorable traps to accumulate. However, helium source rocks have very low generation rates, and the long-distance migration of helium must rely on carriers (mantle-derived fluids, formation water, hydrocarbon fluids, N_2, etc). Driving forces of helium-containing fluid migration are closely related to the types of carriers, either fluid pressure or thermal effect or buoyancy. Collectively, considering their migration pathways, both helium-containing fluids and hydrocarbon fluids follow similar routes, to a certain extent. Prior to their mixture, these two separate fluids employ completely different migration pathways. Migration pathways of helium-containing fluids are not limited to sedimentary strata, and extend to the basement, lower crust, and even lithospheric mantle. Following mixing, they start to migrate together into favorable traps to accumulate.

Regardless of the types of helium gas fields, accumulation conditions for both helium and hydrocarbon gases are considered almost equivalent, and their reservoirs, traps, and caprocks are shared. From the perspective of the petroleum system in its entirety, industrial accumulations of hydrocarbons are found in the depocenters of sedimentary centers, slope zones, and structural high parts (Jia, 2017). However, industrial accumulations of helium occur in (ancient) uplifts and their peripheries. Both helium and hydrocarbon gases accumulate in favorable traps, where the presence of hydrocarbon gases has the following advantages: (1) significantly reducing the partial pressure of helium for helium-containing fluids and favoring the rapid transformation of helium phase from a dissolved state to a free state, which enables efficient helium to enrichment in hydrocarbon gases; and (2) serving as a carrier for helium occurrence and considerably reducing the diffusion property of helium, which causes a decrease in the emission flux of helium.

Helium accumulation involves numerous key scientific issues that should be further investigated, such as the occurrence characteristics of U/Th-rich minerals in helium source rocks, dynamic mechanism of helium release, migration-enrichment pattern of helium, phase-state transition mechanism, diffusion-preservation mechanism, and coupled accumulations of both helium and hydrocarbon gases. Therefore, more research on these key scientific issues will not only enrich and improve the theoretical systems concerning helium enrichment and accumulation in different geological backgrounds but also provide an important scientific basis for delineating more helium resources in China, determining favorable helium-rich zones, and reducing the exploration risk of helium resources.

5. Models of helium accumulation and geological cases

Exploration activities have confirmed that both crust- and mantle-derived helium accumulate on an industrial scale in sedimentary layers. Discovered helium gas pools are mainly crust-derived and crust-mantle complex types. In this regard, diverse types of helium gas fields exhibit notable differences in terms of their geochemical characteristics, migration-enrichment systems, and accumulation mechanisms (Table 7).

Table 7 Comparison of geochemical characteristics between crust-derived and crust-mantle complex helium fields

Type of helium gas pool	Crust-derived type	Crust-mantle complex type
Helium source	Mainly the decay of uranium and thorium minerals	Degassing of mantle-derived fluids and decay of uranium and thorium minerals
Helium isotope	$^3He/^4He$ ratio on the order of 10^{-8}–10^{-7}	$^3He/^4He$ ratio in the magnitude of 10^{-7}–10^{-6}
Migration carrier	Formation water, N_2, Hydrocarbon fluids	Mantle-derived fluids, Formation water, Hydrocarbon fluid, Non-hydrocarbon fluid (CO_2, N_2)
Migration pathway	Mainly basement faults	Lithospheric faults, crustal faults and basement faults
Migration driving force	Diffusion, buoyancy and fluid pressure	Fluid pressure, thermal stress and buoyancy
Enrichment location	(Ancient) Uplift and its periphery	Structural high zone
Accumulation mechanism	Coupled relationships between helium flux and hydrocarbon flux	Coupled relationships among CO_2 loss (dissolution and mineralization), helium flux and hydrocarbon flux
Reservoir age	Mainly Proterozoic and Paleozoic,	Mainly Mesozoic and Cenozoic

	minorly Mesozoic	
Reservoir type	Clastic and carbonate rocks	Clastic, carbonates and volcanic rocks
Type of gas pool	Mainly He-CH_4 and He-N_2 gas pools	Including He-CH_4, He-N_2 and He-CO_2 gas pools
Type of basin	Ancient cratonic basins	Petroliferous basins in tectonically active zones

5.1 Crust-derived helium gas field

Crust-derived helium gas pools are natural gas reservoirs formed by the combined presence of helium (^4He), which is produced by the radioactive decay of U/Th in minerals in helium source rocks, and hydrocarbon gases (mainly CH_4), which are generated by hydrocarbon source rocks under thermal stress. Corresponding model of accumulation is illustrated in Figure 8a. $^3He/^4He$ ratios of crust-derived helium gas pools are typicallyon the order of 10^{-8}, as observed in gas fields such as the Hugoton-Panhandle field, Weiyuan field in the Sichuan Basin, Dongsheng field in the Ordos Basin, Hetianhe field in the Tarim Basin, Dongping field in the Qaidam Basin, and Wufeng-Longmaxi shale field in the Sichuan Basin (Ballentine and Sherwood Lollar, 2002; Liu et al., 2009, 2012; Ni et al., 2014; Cao et al., 2018; Tao et al., 2019; Liu et al., 2021; Zhang et al., 2021; Peng et al., 2022; Nie et al., 2023). Considering the differences in the sources of both helium and hydrocarbon gases, crust-derived helium gas pools are further classified as crust-derived same-source type and crust-derived different-source type.

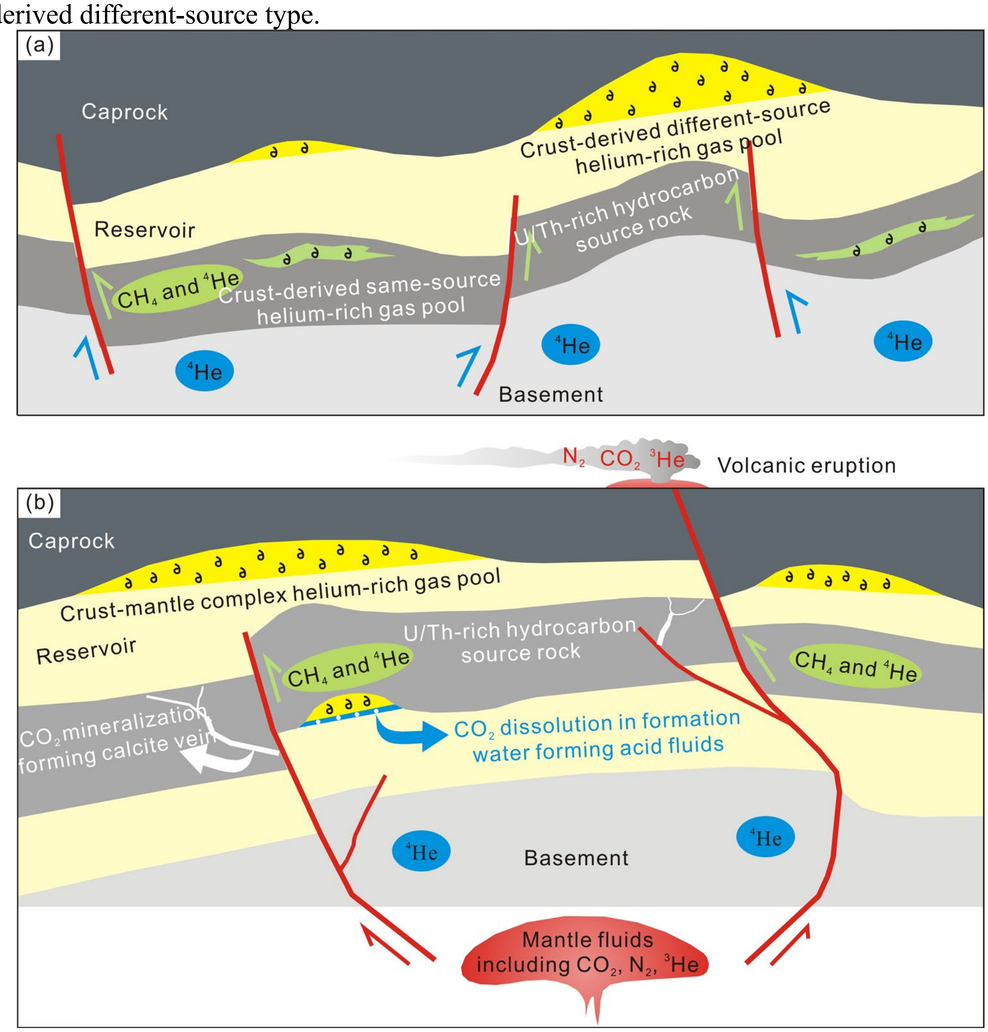

Figure 8 Schematic diagrams of accumulation of various types of helium-rich gas pools. (a) Crust-derived helium gas pools; (b) crust-mantle complex helium gas pools.

5.1.1 Crust-derived same-source helium pools

I. Model of accumulation

Crust-derived same-source type refers to a gas pool where both helium and hydrocarbon gases originate from the same sedimentary rock, which is also known as the self-generation and self-preservation type. This sedimentary rock is commonly composed of either shale or coal seam, which serve as both hydrocarbon source rocks and helium source rocks (with high concentrations of U and Th). Currently, this type of helium gas pool has been discovered in multiple shale layers (i.e., Cambrian, Ordovician, and Silurian) in the Sichuan Basin and its periphery, as well as in the Carboniferous-Permian coal seams in the eastern margin of the Ordos Basin (Liu et al., 2021; Nie et al., 2023).

Helium and shale gas/coalbed methane are known to be in-situ or near-source accumulation. Enrichment of helium results in a dynamic balance between generation and preservation. Helium-supply capacity of shale/coalbed itself is a fundamental requirement for generating an abundant helium flux. Good preservation conditions are vital for the formation of helium-rich gas pools. Episodic hydrocarbon expulsion is a major step in helium loss in shale gas/coalbed methane. In this regard, the timing of episodic hydrocarbon expulsion plays a crucial role in facilitating the subsequent accumulation of helium. For crust-derived same-source helium gas pools, the effective retention of both helium and hydrocarbons within shale/coal plays a key role in the formation of helium-rich natural gases.

II. Geological examples

Abundant helium resources have been discovered within the Cambrian, Ordovician, and Silurian shale-series layers in the Sichuan Basin and its periphery. However, helium concentrations in shale-series layers vary considerably. Cambrian shale layers have relatively high helium concentrations. For example, helium concentrations in shale gas produced in Well W201-H3 (Sichuan Basin), Well Yiye1 (Yichang area), and Well Guidandi1 (Qiandongnan area in Guizhou) are 0.13%, 0.16%, and 0.22%, respectively (Cao et al., 2018; Luo et al., 2019; Dan et al., 2023). However, Wufeng-Longmaxi shale layers exhibit relatively low helium concentrations, approximately 0.04% on average (Chen X J et al., 2023; Qin et al., 2022; Nie et al., 2023). Cambrian shales that are older in age and have high U concentration are believed to be responsible for high helium concentrations in shale gas pools. Studies show that in the middle-upper Yangtze region of China, U concentration in the Cambrian Qiongzhushi/Niutitang shales (10.3–54.9 ppm, 27.90 ppm on average) is approxiamtely three times higher than that in the Upper Ordovician Wufeng Formation to the lower Silurian Longmaxi Formation shales (5.76–14.50 ppm, 9.12 ppm on average) (Zhao et al., 2016).

5.1.2 Crust-derived different-source helium pools

I. Model of accumulation

Crust-derived different-source type refers to a gas pool where helium and hydrocarbon gases have distinct source rocks. Herein, gaseous hydrocarbons are generated from organic matter-rich source rocks (including thermal cracking of ancient oil pools), whereas helium originates from either ancient granite-metamorphic rocks of the basement or hydrocarbon source rocks and bauxite that are rich in U and Th. Almost all explored or commercially minable helium-rich gas fields worldwide are of this type. Crust-derived different-source helium gas pools are mainly distributed in the (paleo) uplift of cratonic basins and their peripheries.

In a relatively long geological period, ancient granite-metamorphic rocks and U/Th-rich sedimentary rocks (mainly hydrocarbon source rocks and bauxite) produce abundant helium flux via decay, which is a fundamental requirement for the formation of helium-rich gas fields. Tectonic uplift causes the formation of fault systems that connect both source rocks and reservoirs, which serve as effective migration pathways for the coupled charging of helium-containing fluids and other hydrocarbons. Good caprock conditions are vital for the optimal preservation of helium-rich gas fields, which are usually composed of well-sealed gypsum, salt, and thick layers of shale (Table 6).

II. Geological examples

Dongsheng gas field in the Ordos Basin consists of a tight sandstone reservoir in the lower Permian Shihezi Formation and a silty mudstone and mudstone caprock in the upper Permian Shihezi Formation. Helium concentration commonly exceeds 0.1% and proven helium reserves are approximately 2×10^8 m³ (He F Q et al., 2022; Peng et al., 2022). Based on the diagram of He concentration versus He/N_2 ratio (Figure 2b), it is inferred that helium in the Dongsheng gas field mainly originates from both bauxite from Carboniferous Benxi Formation and the Carboniferous-Permian coal measure strata (including mudstone and coal). Concentrations of U and Th in both bauxite and coal measure strata are significantly higher than those in the upper crust (Table 8).

Dongsheng gas field experienced multiple episodes of tectonic movements, causing the formation of multiperiod faults with diverse properties and scales (He F Q et al., 2022). During the Caledonian, three first-order main faults formed (Sanyanjing, Wulanjilinmiao, and Boerjianghaizi faults). These three faults extend from the basement to the surface (Peng et al., 2022), which may result in the continuous loss of helium generated from the basement. During the Yanshan and Himalayan periods, many small faults connecting the basement and the upper Paleozoic strata formed, becoming pathways for helium migration. Natural gas in the Dongsheng gas field originates from Carboniferous-Permian coal measure source rocks (Wang et al., 2023). Herein, based on the homogenization temperature of hydrocarbon fluid inclusions from the samples in this zone, the Dongsheng gas field had two periods of hydrocarbon charging: the late stage of the Early Jurassic to the middle stage of the Late Jurassic and the Eocene to the present (Zhao et al., 2017). In summary, considering the regional tectonic evolution and the timing of hydrocarbon charging periods, it is inferred that the coupled accumulation of natural gas and helium primarily occurred from the late stage of the Early Jurassic period to the present.

Table 8 Concentrations of U and Th in the basement, bauxite and coal–measure source rocks in the Dongsheng gas field, Ordos Basin

Types	U concentration (ppm)	Th concentration (ppm)	References
Basement of basin	0.81–2.89/2.59(13)	3.47–8.94/10.71(13)	Wang et al. (2023)
Bauxite from the Carboniferous Benxi Formation	14.45–38.41/24.47(21)	41.21–153.76/82.4(21)	Liu D et al. (2022)
Carboniferous-Permian mudstone	3.59–20.95/6.19(25)	5.76–43.58/21.95(25)	In this study
Carboniferous-Permian coal	1.27–5.05/3.57(3)	3.62–18.56/11.73(3)	Wang et al. (2023)
Upper crust	2.5	10.3	Hans Wedepohl (1995)

Hugoton-Panhandle gas field has helium concentrations of 0.293–1.047% (Balletine and Sherwood Lollar, 2002). Reservoirs of this gas field consist of carbonate rocks from the Permian Chase, Council Grove, and Admire Formations, and the overlying caprock is composed of evaporites from the Permian Leonardian Formation (Rice et al., 1988; Sorenson, 2005; Brown, 2010). Based on the diagram of He concentration versus He/N_2 ratio (Figure 2b), it is inferred that helium in the Hugoton-Panhandle gas field is supplied by both basement granite and hydrocarbon source rocks of the Woodford Formation.

Hydrocarbons in the Hugoton-Panhandle gas field originate from the Woodford shale in the Anadarko Basin. From the Permian to the Paleogene, the Anadarko Basin experienced continuous subsidence. The oil (Permian) and natural gas (Late Cretaceous to Paleogene) that are generated from the Woodford shale are injected into the Panhandle gas field. Amarillo-Wichita Uplift and Laramie orogeny of the Rocky Mountains caused good fault systems to form between basement granite and the Permian carbonate reservoirs, facilitating the optimal migration of helium-containing fluids. In the Neogene, the Permian carbonate strata in eastern Kansas were eroded, and the reservoir pressure of the Hugoton field decreased, causing that natural gases from the Panhandle field to migrate northwards to the Hugoton field. During the Quaternary, the melting of continental glaciers continued eroding the strata, resulting in a steady decrease of reservoir pressure in the Hugoton-Panhandle gas field to approximately 3.1 MPa. Throughout this process, the exsolution of both He and N_2 from formation water led to the formation of helium-rich gas fields (Sorenson, 2005; Brown, 2010).

5.2 Crust-mantle complex helium pools

5.2.1 Model of accumulation

Crust-mantle complex type is a gas pool where the volatiles (e.g., CO_2, N_2, He, H_2, etc.) carried by mantle-derived fluids, helium generated by the decay of U and Th in sedimentary rocks, and hydrocarbon gas generated by hydrocarbon source rocks under thermal stress accumulate together, including in CO_2-He, N_2-He, and CH_4-He gas pools. Crust -mantle complex helium gas fields are commonly distributed in the Mesozoic and Cenozoic basins with active tectonic activities, such as the Songliao Basin, Bohai Bay Basin, Subei Basin, and Sanshui Basin in tectonically active zones of the Eastern China. A model of accumulation for this type of helium gas field is illustrated in Figure 8b.

Due to the influence of plate subduction, accompanied by intense magma and volcanic activities, a series of deep-seated fault zones were found in tectonically active zones, among which faults that cut through the crust and extend into lithospheric became important pathways for mantle-derived fluids to migrate upwards (Wang et al., 2022). As mantle-derived fluids migrate upwards along deep-seated faults, volatiles carried by mantle-derived fluids degas due to abrupt changes in temperature and pressure. Afterwards, they mix with hydrocarbon gases and accumulate in favorable traps. Generally, the closer to deep-seated faults, the greater the impact of mantle-derived fluid activity on gas pools; thus $^3He/^4He$ ratio tends to approach mantle endmember value. This pattern of helium isotopes has been observed in the Eger Graben Rift Zone in the Czech Republic (Weinlich et al., 1999), the Rungwe Volcanic Province in southern Tanzania (Barry et al., 2013), and petroliferous basins in tectonically active zones of the Eastern China (Cao et al., 2001; Feng et al., 2001; Zhang et al., 2008; Zhong, 2017; Ni et al., 2022).

Helium concentrations in gas fields are affected by multiple factors, such as mantle-derived and crust-derived helium fluxes, as well as the degree of loss of active components (mainly CO_2) during the process of the upwards migration of mantle-derived fluids. Both the activity intensity of mantle-derived fluids and the state of deep-seated faults control the flux of mantle-derived helium injected into gas fields. If deep-seated faults extend to the surface and remain open on a geological timescale, continuous emission of helium can result in low helium concentrations in helium gas fields or the inability to form helium gas fields at the peripheries of deep-seated faults. In contrast, if the sealing of regional caprocks is not damaged by the formation of deep-seated faults, the continuous input of mantle-derived volatiles provides a sufficient helium flux for the formation of helium-rich gas fields. In addition, mantle-derived fluids that have very high initial temperatures intrude into sedimentary crustal layers, resulting in a significant increase in temperature around intrusive rocks and promoting the release of crust-derived helium within sedimentary rocks. Mantle-derived fluids contain abundant CO_2, which is an active component. CO_2 is consumed and fixed through dissolution and mineralization during the process of upwards migration of mantle-derived fluids, causing enrichment of both N_2 and He in mantle-derived volatiles.

5.2.2 Geological examples

Since the Neogene, there have been at least five periods of volcanic activities in 501 gas pools in the Huagou Zone in the Jiyang Depression in the Bohai Bay Basin, which provided abundant mantle-derived helium for gas pools. Helium concentrations in these gas pools range from 2.08% to 3.08%, and their $^3He/^4He$ ratios are in the range of 4.34×10^{-6}–4.47×10^{-6}, with a mantle-derived helium contribution of approximately 45% (Cao et al., 2001). However, helium concentrations in gas pools in the Dongpu Depression and Huanghua Depression in the Bohai Bay Basin are between 0.0008% and 0.04%, and their $^3He/^4He$ ratios are in the order of 10^{-7}, where the contribution of mantle-derived helium is generally low, less than 5% in the Dongpu Depression and less than 10% in the Huanghua Depression (Zhang et al., 2008; Ni et al., 2022).

In the Subei Basin, dawsonite (a typical carbonate mineral that forms in a geological environment with a high CO_2 concentration) is commonly found in the Permian oil and gas fields, where the carbon isotopic compositions of dawsonite match those of the mantle-derived CO_2 (Wang et al., 2022). Additionally, calcite veins are found in the overlying mudstone caprocks (Liu Q Y et al., 2023). All evidence indicates that mantle-derived CO_2 is consumed and fixed when migrating upwards to the shallower depths. There are significant differences in N_2/He and CO_2/He ratios between the samples examined from the shallow (below 375 m) and deep (1138–3156.2 m) pools in the Subei Basin. N_2/He and CO_2/He ratios of samples from the shallow depths are low, at 47.01–127.40 and 3.49–16.13, respectively. However, they are larger at greater depths, namely, 5.05–3093.67 and 5.05–47125, respectively (Yang et al., 1991; Guo et al., 1999; Xu et al., 1998).

6 Determination of favorable zones for helium resources in China

Currently, the extracting helium from natural gas is the only viable economic approach with current technologies (Liu Q et al., 2022; Peng et al., 2022). Therefore, zones that are rich in natural gas are also important for the optimized extraction of helium. Determination of favorable zones for helium resources consider both helium concentration and remaining geological reserves of certain gas fields.

Natural gas-rich zones in China are mainly distributed in central and western petroliferous basins, mainly the Ordos Basin, Tarim Basin, and Sichuan Basin (Dai et al., 2007; Li et al., 2020). In recent years, significant breakthroughs have been made in natural gas exploration in continental margin rift basins in the Mesozoic and the Cenozoic, mostly including the Pearl River Mouth Basin, the Qiongdongnan Basin, the Yinggehai Basin, and the East China Sea Basin (Lou et al., 2018; Zhong et al., 2019; Xu et al., 2022). Although natural gas is abundant in offshore, its helium concentration is generally less than 0.01% (He et al., 2005; Dai et al., 2009; Chen et al., 2017), which is unfavorable for commercial extraction.

The Ordos Basin, Tarim Basin, and Sichuan Basin are known for their extremely abundant natural gas resources, with consistent top three rankings in terms of natural gas production for many years. Exploration activities have revealed that natural gas in these three basins typically contains helium, but helium concentrations vary considerably (Table 9).

In the Ordos Basin, six gas fields (Dongsheng, Qingyang, Qingshimao, Yichuan, Zhengning, Huanglong) have helium concentrations above the threshold of commercial helium extraction (0.05%). Among them, helium cocentrations in the Dongsheng, Qingyang, Zhengning, and Huanglong gas fields exceeds 0.1%. Thus, these gas fields are important targets for the implementation of commercial extraction in the Ordos Basin. Although the Sulige gas field has lower helium concentrations, approximately 0.04% (comparable to the North Par gas field in Qatar), its proven natural gas reserves and annual production are known to be the largest in the Ordos Basin, making it commercially valuable for helium extraction.

In the Tarim Basin, several gas fields in the Maigaiti Slope and peripheral areas have abundant helium, with helium concentrations ranging from 0.1% to 0.4%. Therefore, these gas fields are important targets for commercial extraction of helium in the Tarim Basin.

Multiple large gas fields in the Sichuan Basin (i.e., Anyue, Yuanba, Puguang, Hechuan) generally have low helium concentrations and therefore are insufficient for the commercial production of helium. Only seven small to medium gas fields (Tongnanba, Wenquanjing, Leiyingpu, Huangcaoxia, Shaguanping, Xiangguosi, and Shuanglong) have helium concentrations above the commercial threshold for extraction; thus, these gas fields are important targets for commercial extraction of helium in the Sichuan Basin. Additionally, shale gas resources in the Sichuan Basin and its periphery are extremely abundant, and shale gas commonly contains helium. Helium concentrations in shale gas from the Wufeng-Longmaxi Formations in the Fuling, Weiyuan, Fushun-Yongchuan zones are approximately 0.04%, whereas in the Pengshui zone, they are approximately 0.1% (Nie et al., 2023). Helium concentration from the Cambrian shale gas in the Sichuan Basin and its periphery exceeds 0.1% (Cao et al., 2018; Luo et al., 2019; Dan et al., 2023). This indicates that future exploration efforts aimed at identifying helium resources should focus more on these two shale strata.

Natural gas production in the Qaidam Basin has been maintained at a level of 6×10^9 m^3 for over a decade, a level that is far below that of the Ordos, Sichuan, and Tarim Basins. However, the Dongping, Mabei, and Jianbei gas fields in the northern margins of the Qaidam Basin exhibit good helium grades, with helium concentrations exceeding 0.25% on average. Therefore, these three gas fields are important targets for industrial helium extraction in the Qaidam Basin. In addition, during exploration efforts targeting coal resources, the desorption of gases from retrieved shale cores of the Jurassic Daheishan Formation in the Tuanyushan zone revealed helium concentrations ranging from 0.5% to 1.14%. Additionally, the desorption of gases during drilling into the Paleogene and Neogene interlayered sandstone-mudstone sections in the Quanjishan area yielded a helium concentration of 1.1%, notably surpassing the threshold for commercial extraction of helium. These findings underscore the importance of focusing on exploration efforts targeting helium resources in these areas.

China's helium-related industries are currently in a critical stage of technological exploration and development, with a focus on scaling up helium extraction from helium-rich natural gas. Despite significant advancements in this area, extracting low-abundance helium from natural gas still poses significant challenges. Comprehensively considering China's helium grade, helium resource endowment, natural gas industrialization process, and current helium purification processes, priority zones for future operations and helium extraction efforts include the helium-rich gas fields (He≥0.1%) in the four basins mentioned above. Additionally, certain (super) large helium-containing gas fields (He=0.05–0.1%) serve as important replacement zones.

Table 9 Helium concentrations in the natural gas fields in major petroliferious basins in the central and western China

Basin	Gas field	Helium concentration	References
Ordos	Dongsheng	0.13%	Peng et al. (2022)
	Qingyang	＞0.1%	In this study
	Qingshimao	＞0.05%	
	Yichuan	Approximately 0.05%	
	Zhengning	Approximately 0.2%	
	Huanglong	0.23%	
	Sulige	Approximately	Dai et al. (2014); Liu Q et al. (2022)
	Daniudi	0.04%	
	Jingbian	Approximately	
	Zizhou	0.02%	
	Shenmu		
	Yulin		
	Mizhi		
Tarim	Akemomu	＞0.1%	In this work
	Hetianhe	＞0.3%	
	Luosi	＞0.2%	Tao et al. (2019)
Sichuan	Weiyuan	＞0.2%	Ni et al. (2014); Qin et al., (2022)
	Tongnanba	Approximately 0.06%	Dai et al. (2013)
	Wenquanjing	0.05%	Song (2014)
	Leiyinpu	Approximately 0.08%	Ni et al. (2014)
	Huangcaoxia	Approximately 0.05%	Wu et al. (2013); Ni et al. (2014)
	Shaguanping	0.05%	
	Xiangguosi	0.06%	Wu et al. (2013)
	Shuanglong	0.15%	
	Fuling shale gas	Approximately 0.04%	Nie et al. (2023)
	Weiyuan shale gas	Approximately 0.04%	
	Yongchuan shale gas	Approximately 0.04%	
	Pengshui shale gas	Approximately 0.1%	
Qaidam	Dongping	＞0.3%	Zhang et al. (2020)
	Mabei	0.26%	Zhang et al. (2019); Han et al., (2020); He Z Y et al. (2022)
	Jianbei	0.29%	Zhang et al. (2020); He Z Y et al. (2022)

7. Conclusions

Through the analysis of key factors of accumulation and enrichment patterns observed in representative helium-rich gas fields worldwide, the following points have been observed:

(1) Helium in natural gas exhibits "scarce", "accompanying", and "complex" properties. Helium-rich gas fields are primarily found in uplifted zones of ancient cratonic basins and their

peripheries, typically at depths <4500 m. These zones are characterized by well- developed fault systems, relatively low reservoir pressures, and limited hydrocarbon charging, which create favorable conditions for helium accumulation.

(2) Based on differences in their helium isotopes ($^3He/^4He$), helium fields can be divided into two types: crust-derived and crust-mantle complex types. According to the diagram of He concentration versus He/N_2 ratio, three models of helium supply for crust-derived helium fields have been identified: basement, combined basement-sedimentary rock, and sedimentary rock helium supply types.

(3) There are notable disparities in the origins and migration patterns between helium and gaseous hydrocarbons. Helium necessitates carriers (formation water, hydrocarbon fluids, N_2, and mantle-derived fluids, etc.) during both accumulation and long-distance migration processes, where migration conduits are not confined to sedimentary strata, and may extend to the basin's basement, lower crust, and even lithospheric mantle. However, accumulation conditions for helium (reservoir, trap and caprock) are considered nearly equivalent to those for gaseous hydrocarbons.

(4) The formation of helium-rich gas fields requires the optimal combination of multiple key factors of accumulation. An abundant helium flux is a fundamental condition for the formation of helium-rich gas fields. Fault systems that connect source-reservoir systems are considered effective pathways for the coupled charging of helium-containing and hydrocarbon fluids. Presence of gaseous hydrocarbons facilitates both the rapid exsolution of helium in helium-containing fluids and subsequent effective aggregation in gaseous hydrocarbons; moreover, the presence of gaseous hydrocarbons reduces both reduces the diffusion of helium and diminishes its escape flux. Good caprock conditions are vital for the optimal preservation of helium-rich gas fields over geological timescales.

(5) In terms of helium grade, helium resource endowment, natural gas industrialization process, and current helium purification technologies, helium-rich gas fields (He⩾0.1%) of the Ordos, Tarim, Sichuan, and Qaidam Basins in central and western China are priority zones for the deployment of commercial helium production. Additionally, certain (super) large helium-containing gas fields (He=0.05–0.1%) can serve as important replacement zones.

Acknowledgements

This work was supported by the National Natural Science Foundation of China (Grant Nos. 42203027, 42141021, U2244209, U20B6001, 42172149, and 42311530064), the China Postdoctoral Science Foundation (Grant No. 2023M730039), and the China National Petroleum Corporation Limited-Peking University Basic Research Program (Grant No. JTGS-2022-JS-327).

References

Abrosimov V K, Lebedeva E Yu. 2013. Solubility and Thermodynamics of Dissolution of Helium in Water at Gas Partial Pressures of 0.1–100 MPa within a Temperature Range of 278–353 K. Russ J Inorg Chem, 58: 808–812.

Anderson S T. 2018. Economics, helium, and the U.S. federal helium reserve: summary and outlook. Nat Resour Res, 27: 455–477.

Bähr Roland, Lippolt Hans J., Wernicke Rolf S. 1994. Temperature-induced ^{4}He degassing of specularite and botryoidal hematite: A ^{4}He retentivity study. J Geophys Res-Sol Ea, 99: 17695–17707.

Ballentine C J, Burgess R, Marty B. 2002. Tracing fluid origin, transport and interaction in the crust. Rev Miner Geochem, 47: 539–614.

Ballentine C J, Burnard P G. 2002 Production, release and transport of noble gases in the continental crust. Rev Miner Geochem, 47: 481–538.

Ballentine C J, Sherwood Lollar B. 2002. Regional groundwater focusing of nitrogen and noble gases into the Hugoton-Panhandle giant gas field, USA. Geochim Cosmochim Acta, 66: 2483–2497.

Barry P H, Hilton D R, Fischer T P, de Moor J M, Mangasini F, Ramirez C. Helium and carbon isotope systematics of cold "mazuku" CO_2 vents and hydrothermal gases and fluids from Rungwe Volcanic Province, southern Tanzania. Chem Geol, 2013, 339: 141-156.

Barry P H, Lawson M, Meurer W P, Danabalan D, Byrne D J, Mabry J C, Ballentine C J. 2017. Determining fluid migration and isolation times in multiphase crustal domains using noble gases. Geology ,45: 775–778.

Barry P H, Lawson M, Meurer W P, Warr O, Mabry J C, Byrne D J, Ballentine C J. 2016. Noble gases solubility models of hydrocarbon charge mechanism in the Sleipner Vest gas field. Geochim Cosmochim Acta ,194: 291–309.

Battani A, Sarda P, Prinzhofer A. 2000. Basin scale natural gas source, migration and trapping traced by noble gases and major elements: the Pakistan Indus basin. Earth Planet Sci Lett ,181: 229–249.

Becker T P, Lynds R. 2012. A geologic deconstruction of one of the world's largest natural accumulations of CO_2, Moxa arch, southwestern Wyoming. AAPG Bull, 96: 1643–1664.

Bergfeld D, Evans W C., Hunt A G, Lopez T, Schaefer J R. 2020. A post-eruption study of gases and thermal waters at Okmok volcano, Alaska. J Volcanol Geoth Res, 396: 106853.

Boyce J W, Hodges K V, Olszewski W J, Jercinovic M J. 2005. He diffusion in monazite: Implications for (U–Th)/He thermochronometry. Geochem Geophy Geosy, 6: Q12004.

Broadhead R F. 2005. Helium in New Mexico—geologic distribution, resource demand, and exploration possibilities. New Mexico Geol, 27: 93–100.

Brown A A. 2017. Possible origins for low thermal maturity, high-nitrogen natural gases. AAPG Annual Convention and Exhibition Article, #90291.

Brown A. 2019. Origin of helium and nitrogen in the Panhandle-Hugoton field of Texas, Oklahoma, and Kansas, United States. AAPG Bull, 103: 369–403.

Brown Alton A. 2010. Formation of High Helium Gases: A Guide for Explorationists. AAPG Conference, 1–14.

Byrne D J, Barry P H, Lawson M, Ballentine C J. 2018. Determining gas expulsion vs retention during hydrocarbon generation in the Eagle Ford Shale using noble gases. Geochim Cosmochim Acta, 241: 240–254.

Cai Z, Clarke R H, Glowacki B A, Nuttall W J, Ward N. 2010. Ongoing ascent to the helium production plateau-Insights from system dynamics. Resour Policy, 35: 77–89.

Cao C, Zhang M, Tang Q, Yang Y, Lv Z, Zhang T, Chen C, Yang H, Li L. 2018. Noble gas isotopic variations and geological implication of Longmaxi shale gas in Sichuan Basin, China. Mar Petrol Geol, 89: 38–46.

Cao Z X, Che Y, Li J L, Li H W. 2001. Accumulation analysis on a helium-enriched gas reservoir in huagou area, the jiyang depression (in Chinese). Petrol Geol Exp, 23: 395–399.

Chen H H, Mi L J, Liu Y H, Han J Y, Kong L T. 2017. Genesis, distribution and risk belt prediction of CO_2 in deep-water area in the Pearl River Mouth Basin (in Chinese). Acta Petrol Sin, 38: 119–134.

Chen J F, Liu K X, Dong Q W, Wang H, Luo B, Dai X. 2021. Research status of helium resources in natural gas and prospects of helium resources in China (in Chinese). Nat Gas Geosci, 32: 1436–1449.

Chen J F, Xu J, Wang J, Liu P, Chen F R, Li M W. 2023. Paleo-environmental variation and its control on organic enrichment in the black rock series, Cambrian Yuertusi Formation in Northwest Tarim Basin (in Chinese). Earth Sci Front, 30: 150–161.

Chen J F, Xu Y C, Huang D F. Geochemical Characteristics and Origin of Natural Gas in Tarim Basin, China. AAPG Bull, 2000, 84: 591-606.

Chen X J, Chen G, Bian R K, Du W. 2023.The helium resource potential and genesis mechanism in Fuling shale gas field, Sichuan Basin (in Chinese). Nat Gas Geosci, 34: 469–476.

Cheng A R, Sherwood Lollar B, Gluyas J G, Ballentine C J. 2023. Primary N_2–He gas field formation in intracratonic sedimentary basins. Nature, 615: 94–99.

Cherniak D J, Watson E B, Thomas J B. 2009. Diffusion of helium in zircon and apatite. Chem Geol, 268: 155–166.

Civan F. 2010. Effective Correlation of Apparent Gas Permeability in Tight Porous Media. Transport Porous Med, 82: 375–384.

Crovetto R, Fernández-Prini R, Japas M L. 1982. Solubilities of inert gases and methane in H_2O and in D_2O in the temperature range of 300 to 600 K. J Chem Phys, 76(2): 1077–1086.

Dai J F, Hu G Y, Ni Y Y, Li J, Luo X, Yang C, Hu P A, Zhou Q H. 2009. Distribution Characteristics of Natural Gas in Eastern China (in Chinese). Nat Gas Geosci, 20: 471–487.

Dai J X, Chen J F, Zhong N N, Pang X Q, Qin S F. 2003. China's large gas fields and their gas sources (in Chinese). Beijing: Science Press.

Dai J X, Liao F R, Ni Y Y. 2013. Discussions on the gas source of the Triassic Xujiahe Formation tight sandstone gas reservoirs in Yuanba and Tongnanba, Sichuan Basin: An answer to Yinfeng et al (in Chinese). Petrol Explor Dev, 40: 250–256.

Dai J X, 2014 OG

Dai J X, Zou C N, Tao S Z, Liu Q Y, Zhou Q H, Hu P A, Yang C. 2007. Formation conditions and main controlling factors of large gas fields in China (in Chinese). Nat Gas Geosci,18: 473–484.

Dai J, Ni Y, Qin S, Huang S, Gong D, Liu D, Feng Z, Peng W, Han W, Fang C. 2017. Geochemical characteristics of He and CO_2 from the Ordos (cratonic) and Bohaibay (rift) basins in China. Chem Geol, 469: 192–213.

Dai Jingxin, Yang Shufeng, Chen Hanlin, Shen Xiaohua. 2005. Geochemistry and occurrence of inorganic gas accumulations in Chinese sedimentary basins. Organic Geochemistry, 36: 1664–1688.

Dan Y, Yan J F, Bao S J, Liang B, Ma L, Nie G Q, Cao J F, Ji S C, Han K. 2023. Discovery of Sinian-Cambrian multi-tier shale gas in Guidandi-1 well of southwest margin of Xuefeng uplift. Geology in China, 50: 291-292.

Danabalan D, Gluyas J G, Macpherson C G, Abraham-James T H, Bluett J J, Barry P H, Ballentine C J. 2022. The principles of helium exploration. Petrol Geosci, 28: 2021–2029.

Danabalan D. 2017. Helium: Exploration Methodology for a Strategic Resource. Doctoral Dissertation. Durham: Durham University.

Dodson M H. 1973. Closure temperature in cooling geochronological and petrological system. Contrib Mineral Petrol, 40: 259–274.

Dubois M K, Byrnes A P, Bhattacharya S, Bohling G C, Deveton J H, Barba R E. 2007. Hugoton Asset Management Project (HAMP): Hugoton Geomodel Final Report. Kansas Geological Survey, 2007-6-1.

Dunai T L, Roselieb K. 1996. Sorption and diffusion of helium in garnet: implications for volatile tracing and dating. Earth Planet Sci Lett, 139: 411–421.

Elliot T, Ballentine C J, O'Nions R K, Ricchiuto T. 1993. Carbon, helium, neon and argon isotopes in a Po basin (northern Italy) natural gas field. Chem Geol, 106: 429–440.

Farley K A. 2000. Helium diffusion from apatite: General behavior as illustrated by Durango fluorapatite. J Geophys Res-Sol Earth, 105: 2903–2914.

Farley K A. 2002. (U–Th)/He dating: Techniques, calibrations, and applications. Rev Mineral Geochem, 47: 819–844.

Feng Z H, Huo Q L, Wang X. A study of helium reservoir formation characteristic in the north part of Songliao Basin (in Chinese). Nat Gas Industry, 21: 27–30.

Feng Z. 2008. Volcanic rocks as prolific gas reservoir: A case study from the Qingshen gas field in the Songliao Basin, NE China. Mar Petrol Geol, 25: 416–432.

Fu X T, Wang Z P, Lu S F. 1996. Mechanisms and solubility equations of gas dissolving in water. Sci China Ser B-Chem, 39: 500–508.

Geert K, Afifi A M, Al-Hajri Sa'id A, Droste H J. 2001. Paleozoic Stratigraphy and Hydrocarbon Habitat of the Arabian Plate. GeoArabia, 6: 407–442.

Gilfillan Stu M V, Ballentine Chris J, Holland Greg, Blagburn Dave, Sherwood Lollar Barbara, Stevens Scott, Schoell Martin, Cassidy Martin. 2008. The noble gas geochemistry of natural CO_2 gas reservoirs from the Colorado Plateau and Rocky Mountain provinces, USA. Geochim Cosmochim Acta, 72: 1174–1198.

Guélard J, Beaumont V, Rouchon V, Guyot F, Pillot D, Jézéquel D, Ader M, Newell K D, Deville E. 2017. Natural H_2 in Kansas: Deep or shallow origin? Geochem Geophy Geosy, 18: 1841–1865.

Guo N F, You X Z, Xu J. 1999.Geological character of Xiqiao helium bearing gas field and prospecting of helium bearing natural gas in North Jiangsu basin (in Chinese). Petrol Explor Dev, 26: 24–26.

Guo X S, Hu D F. Wei Z H, Li Y P, Wei X F. 2016. Discovery and exploration of Fuling shale gas field (in Chinese). China Petrol Explor, 21: 24–37.

Halford D T, Karolytė R, Barry P H, Whyte C J, Darrah T H, Cuzella J J, Sonnenberg S A, Ballentine C J. 2022. High helium reservoirs in the Four Corners area of the Colorado Plateau, USA. Chem Geol, 596: 120790.

Han W, Liu W J, Li Y H, Zhou J L, Zhang W, Zhang Y P, Chen X H, Huang B. 2020. Characteristics of rare gas isotopes and main controlling factors of radon enrichment in the northern margin of Qaidam Basin (in Chinese). Nat Gas Geosci, 31: 385–392.

Han Y H, Luo H Y, Xue Y Z, Li X F, Zhang T H, Zhang Y P, Tao P F. 2022. Genesis and helium enrichment mechanism of geothermal water-associated gas in Weihe Basin (in Chinese). Nat Gas Geosci, 33: 277–287.

Hand E. 2016. Massive helium fields found in rift zone of Tanzania. Science, 353: 109–110.

Hans Wedepohl K. 1995. The composition of the continental crust: Geochim Cosmochim Acta, 59: 1217–1232.

He D X, Chen J F, Zhang C, Li W, Zhou J X. Compositions of non-hydrocarbon and noble gases in natural gas samples from Tarim Basin, China. Geochem J, 2015, 49: 271-282.

He D X, Tang Y J, Hu J J, Mo S W, Chen J F. 2020. Geochemical characteristics of noble gases in natural gases from the Tarim Basin (in Chinese). Oil Gas Geol, 41: 755–762.

He F Q, Wang F B, Wang J, Zou Y R, An C, Zhou X Y, Ma L B, Zhao Y Q, Zhang J, Liu D M, Jiang H J.2022. Helium distribution of Dongsheng gas field in Ordos Basin and discovery of a super large helium-rich gas field (in Chinese). Petrol Geol Exp, 44: 1–10.

He J X, Xia B, Liu B M, Zhang S L. 2005. Analysis of the genesis and migration and accumulation of CO_2 and controlling factors in the onland and offshore areas of eastern China (in Chinese). Geol China, 32: 663–673.

He Z Y, Yang G J, Zhou J L, Li Y H, Zhang W, He W F, Zheng B, Han W, Ma S W. 2022. Helium Enrichment Law and Predication of Prospective Areas of the North Qaidam Basin (in Chinese). Northwest Geol, 55: 45-60.

Holail H M, Kolkas M M, Friedman G M. 2006. Facies analysis and petrophysical properties of the lithologies of the north gas field, Qatar. Carbonate Evaporite, 21: 40–50.

Jai C Z. 2017. Breakthrough and significance of unconventional oil and gas to classica' petroleum geological theory (in Chinese). Petrol Explor Dev, 44: 1–11.

Keir R S. 2010. A note on the fluxes of abiogenic methane and hydrogen from mid-ocean ridges. Geophys Res Lett, 37: L24609.

Kennedy B Mack, van Soest M C. 2006. A helium isotope perspective on the Dixie Valley, Nevada, hydrothermal system. Geothermics, 35: 26–43.

Li J Y, Li Y H. Hu S H, Zhou J L, Chen G C, Zhang S Q. 2022. "Shanxi-type" helium accumulation model and its essentiality (in Chinese). J Xi'an Univ Sci Technol, 42: 529–536.

Li P P, Zhang X D, Zhang S. 2018. Response of methane diffusion in varying degrees of deformed coals to different solvent treatments. Curr Sci, 115: 2155–2161.

Li S Z, Suo H Y, Dai L M, Liu L P, Jin C, Liu X, Hao T Y, Zhou L H, Liu B H, Zhou J T, Jiao Q. 2018. Development of the Bohai Bay Basin and destruction of the North China Craton (in Chinese). Earth Sci Front,17: 64–89.

Li Y H, Li J Y, Zhou J L, Zhao F H, Xu D. 2022. Research Progress and New Views on Evaluation of Helium Resources (in Chinese). J Earth Sci Environ, 44: 363–373.

Li Y H, Zhang W, Wang L, Zhao F H, Han W, Chen G C. 2017. Henry's Law and accumulation of crust-derived helium: A case from Weihe Basin, China (in Chinese). Nat Gas Geosci, 28: 495–501.

Li Y H, Zhou J L, Zhang W. 2018. Helium reservoir formation conditions and resource prospects in Weihe Basin (in Chinese). Beijing: Science Press.

Li Y, Cao C H, Hu H Y, Huang H F. 2022. The Use of Noble Gases to Constrain Subsurface Fluid Dynamics in the Hydrocarbon Systems. Front Earth Sci, 10, 1–12.

Li Y, Xue Z J, Cheng Z, Jiang H J, Wang R Y. 2020. Progress and development directions of deep oil and gas exploration and development in China (in Chinese). China Petrol Explor, 25: 45–57.

Lippolt H J, Leitz M, Wernicke R S, Hagedorn B. 1994. (Uranium+thorium)/helium dating of apatite: experience with samples from different geochemical environments. Chem Geol, 112: 179–191.

Lippolt H J, Weigel E. 1988. ^{4}He diffusion in ^{40}Ar retentive minerals. Geochim Cosmochim Acta, 52: 1449–1458.

Liu C, Sun B L, Zeng F G, Chang X D, Guo S Q, Wang Y H, Liu Y F, Zhang S W, Chen J W, Li J. 2021. Discovery and origin of helium-rich gas on the Shixi area, eastern margin of the Ordos Basin (in Chinese). J China Coal Soc, 46: 1280–1287.

Liu D, Zhang H T, Yang X M, Zhao T P, Kou X P, Zhu B D. 2022. Well Logging Evaluation of Bauxite Reservoirs in Ordos Basin (in Chinese). Xinjiang Petrol Geol, 43: 261–270.

Liu F J. 1992. Research progress of light hydrocarbon diffusion in cap beds and diffusion failure estimation of Sinian gas reservoirs in Weiyuan Gas field, Sichuan Province (in Chinese). Nat Gas Geosci, 5: 11–16.

Liu H. 2021. Correlation analysis of mesozoic high U, Th granites in northern Qinling and helium accumulation area in Wei river basin (in Chinese). Ground Water, 43: 152–154.

Liu K X, Chen J F, Fu F, Wang H, Luo B, Dai X, Yang J J. 2022. Discussion on distribution law and controlling factors of helium-rich natural gas in Weiyuan gas field (in Chinese). J China Univ Petrol (Ed Nat Sci), 46: 12–21.

Liu K X, Chen J F, Fu R, Wang H, Luo B, Chen Z Y, Dong Q W, Dai X, Zhang B S. 2023. Distribution characteristics and controlling factors of helium-rich gas reservoirs. Gas Sci Eng, 110, 204885.

Liu Q Y, Dai J X, Jin Z J, Li J, Zhou Q H, Feng Z H, Sun H J. 2014. Abnormal hydrogen isotopes of natural gases from the Qingshen gas field, the Songliao Basin (in Chinese). Geochim, 43: 460–468.

Liu Q Y, Dai J X, Jin Z J, Li J. 2009. Geochemistry and Genesis of Natural Gas in the Foreland and Platform of the Tarim Basin (in Chinese). Acta Geol Sin, 83: 107–114.

Liu Q Y, Dai J X, Jin Z J, Li J, Wu X Q, Meng Q Q, Yang C, Zhou Q H, Feng Z H, Zhu D Y. 2016. Abnormal carbon and hydrogen isotopes of alkane gases from the Qingshen gas field, Songliao Basin, China, suggesting abiogenic alkanes? J Asian Earth Sci, 115: 285–297.

Liu Q Y, Jin Z J, Chen J F, Krooss B M, Qin S F. 2012. Origin of nitrogen molecules in natural gas and implications for the high risk of N_2 exploration in Tarim Basin, NW China. J Petrol Sci Eng, 81: 112–121.

Liu Q Y, Jin Z J, Li H L, Wu X Q, Tao X W, Zhu D Y, Meng Q Q. 2018. Geochemistry characteristics and genetic types of natural gas in central part of the Tarim Basin, NW China. Mar Petrol Geol, 89: 91–105.

Liu Q Y, Jin Z J, Meng Q Q, Wu X Q, Jia H C. 2015. Genetic types of natural gas and filling patterns in Daniudi gas field, Ordos Basin, China. J Asian Earth Sci, 107: 1–11.

Liu Q Y, Wu X Q, Jia H C, Ni C H, Zhu J H, Miao J J, Zhu D Y, Meng Q Q, Peng W L, Xu H Y. 2022. Geochemical characteristics of helium in natural gas from the Daniudi Gas Field, Ordos Basin, Central China. Front Earth Sci, 10: 823308.

Liu Q Y, Zhu D Y, Jin Z J, Meng Q Q, Wu X Q, Yu H. 2017. Effects of deep CO_2 on petroleum and thermal alteration: The case of the Huangqiao oil and gas field. Chem Geol, 469: 214–229.

Liu Q Y, Zhu D Y, Jin Z J, Tian H L, Zhou B, Jiang P X, Meng Q Q, Wu X Q, Xu H Y, Hu T, Zhu H X. 2023. Carbon capture and storage for long-term and safe sealing with constrained natural CO_2 analogs. Renew Sust Energ Rev, 171: 113000.

Liu S G, Ma Y S, Sun W, Cai X Y, Liu S, Huang W M, Xu G S, Yong Z Q, Wang G Z, Wang H, Pan C L. 2008. Studying on the Differences of Sinian Natural Gas Pools between Weiyuan Gas Field and Ziyang Gas-Brone Area, Sichuan Basin (in Chinese). Acta Geol Sin, 82: 328–337.

Liu Y H, Li R L, Zhao H W, Wang W, Wang X F, Cao C H. 2017. Characteristics of deep large fault and its effects on gas accumulation: A case study on Wanjinta area in Dehui fault depression of the Songliao Basin (in Chinese). Nat Gas Explor Dev, 40: 23–31.

Liu Y T, Duan K, Zhang X B, Hu Y Y, Ma D Z, Tao H F. 2023. Formation conditions of helium-rich gas in bedrock reservoirs: Taking Dongping Gas Field in Qaidam Basin and Panhandle-Hugoton Gas Field in central United States as examples (in Chinese). Nat Gas Geosci, 34: 618–627.

Lou Y, Pan J P, Wang L X, Wang S Y. 2018. Problems and countermeasures in the exploration and development of natural gas resources in China (in Chinese). Int Petrol Econ, 26: 21–27.

Luo S Y, Chen X H, Liu A, Li H. 2019. Geochemical features and genesis of shale gas from the Lower Cambrian Shuijingtuo Formation shale in Yichang block, Middle Yangtze region (in Chinese). Oil Gas Geol, 40: 999–1010.

Lupton G L. 1983. Terrestrial inert gases: isotope tracer studies and clues to primordial components in the mantle. Annu Rev Earth Pl Sci, 11(1): 371–414.

Lyu X, Jiang Y. 2017. Genesis of Paleogene gas in the Dongpu Depression, Bohai Bay Basin, East China. J Petrol Sci Eng, 156: 181–193.

Meng B K, Zhou S X, Li J, Sun Z X. 2021. Helium potential evaluation of different types of rocks in the Upper Yangtze region and theoretical calculation of helium recovery conditions for shale in Upper Yangtze region (in Chinese). Mineral Petrol, 41: 102–113.

Ni C H, Wu X Q, Liu Q Y, Zhu D Y, Yang F, Meng Q Q, Xu H Y, Xu S T, Xu T W. 2022. Helium signatures of natural gas from the Dongpu Sag, Bohai Bay Basin, Eastern China. Front Earth Sci, 10: 862677.

Ni Y Y, Dai J X, Tao S Z, Wu X Q, Liao F R, Wu W, Zhang D J. 2014. Helium signatures of gases from the Sichuan Basin, China. Org Geochem, 74: 33–43.

Nie H K, Liu Q Y, Dang W, Li P, Su H K, Bao H Y, Xiong L, Liu Z J, Sun C X, Zhang P X. 2023. Enrichment mechanism and resource potential of shale-type helium: A case study of Wufeng Formation-Longmaxi Formation in Sichuan Basin. Sci China Earth Sci, 66: 1279–1288.

Oxburgh E R, O'Nions R K, Hill R I. 1986. Helium isotopes in sedimentary basins. Nature, 324: 632–635.

Ozima M, Podosek F A. 1983. Noble gas Geochemistry. Cambridge: Cambridge University Press.

Peng W L, Liu Q Y, Zhang Y, Jia H C, Zhu D Y, Meng Q Q, Wu X Q, Deng S, Ma Y S. 2022. The first extra-large helium-rich gas field identified in a tight sandstone of the Dongsheng Gas Field, Ordos Basin, China (in Chinese). Sci China Earth Sci, 52: 1078–1085.

Porcelli D, Ballentine C J. 2002. Models for the distribution of Terrestrial noble gases and the evolution of the atmosphere. Rev Mineral Geochem, 47: 411–480.

Pordea R J, Jenden P D, Kaplan I R, Craig H. 1986. Mantle helium in Sacramento basin natural gas wells. Geochim Cosmochim Acta, 50: 2847–2853.

Potter R W, Clynne M A. 1978. The solubility of the noble gases He, Ne, Ar, Kr, and Xe in water up to the critical point. J Solution Chem, 7: 837–844.

Pray H A, Schweickert C E, Minnich B H. 1952. Solubility of hydrogen, oxygen, nitrogen, and helium in water at elevated temperatures. Industrial & Engineering Chemistry, 44: 1146–1151.

Qin S F, Li J Y, Wang J M, Tao G, Wang X F. 2022. Helium enrichment model of helium-rich gas reservoirs in petroliferous basins in China (in Chinese). Nat Gas Ind, 42: 125–134.

Rafik B, Kamel B. 2017. Prediction of permeability and porosity from well log data using the nonparametric regression with multivariate analysis and neural network, Hassi R'Mel Field, Algeria. Egypt J Petrol, 26: 763–778.

Ranta E, Halldórsson S A, Barry P H, Ono S, Robin J G, Kleine B I, Ricci A, Fiebig J, Sveinbjörnsdóttir Á E, Stefánsson A. 2023. Deep magma degassing and volatile fluxes through volcanic hydrothermal systems: Insights from the Askja and Kverkfjöll volcanoes, Iceland. J Volcanol Geoth Res, 436: 107776.

Reich M, Ewing R C, Ehlers T A, Becker U. 2007. Low-temperature anisotropic diffusion of helium in zircon: implications for zircon (U–Th)/He thermochronometry. Geochim Cosmochim Acta, 71: 3119–3130.

Reiners P W, Farley K A. 1999. Helium diffusion and (U–Th)/He thermochronometry of titanite. Geochim Cosmochim Acta, 63: 3845–3859.

Reiners P W. 2005. Zircon (U–Th)/He thermochronometry. Rev Mineral Geochem 58: 151–179.

Rice D D, Threlkeld C N, Vuletich A K. 1988. Character, origin and occurrence of natural gases in the Anadarko basin, southwestern Kansas, western Oklahoma and Texas Panhandle, U.S.A. Chem Geol, 71: 149–157.

Sakata S, Takahashi M, Hoshino K. 1986. Geochemical study on genesis of natural gases accumulated in deep volcaniclastic rocks. Journal of the Japanese Association for Petroleum Technology, 51: 228–238. (In Japanese with English Abstract)

Sano Y, Notsu K, Ishibashi Jun-ichiro, Igarashi G, Wakita H. 1991. Secular variations in helium isotope ratios in an active volcano: Eruption and plug hypothesis. Earth Planet Sci Lett: 107: 95–100.

Sathaye K J, Larson T E, Hesse M A. 2016. Noble gas fractionation during subsurface gas migration. Earth Planet Sci Lett, 450: 1–9.

Sherwood Lollar B, Frape S, Weise S, Macko S, Welhan J. 1993. Abiogenic methanogenesis in crystalline rocks. Geochim Cosmochim Acta, 57: 5087–5097.

Sherwood Lollar B, Lacrampe-Couloume G, Voglesonger K, Onstott T, Pratt L, Slater G. 2008. Isotopic signatures of CH_4 and higher hydrocarbon gases from Precambrian Shield sites: A model for abiogenic polymerization of hydrocarbons. Geochim Cosmochim Acta, 72, 4778–4795.

Shuster D L, Flowers R M, Farley K A. 2006. The influence of natural radiation damage on helium diffusion kinetics in apatite. Earth Planet Sci Lett, 249: 148–161.

Song L. 2014. Dynamic analysis of Wenquanjing carboniferous gas reservoir (in Chinese). Master's Dissertation. Chengdu: Southwest Petroleum University.

Sorenson R P. 2005. A dynamic model for the Permian Panhandle and Hugoton fields, western Anadarko Basin. AAPG Bull, 89: 921–938.

Sun Z X, Li P P, Zhou S X. 2023. A laboratory observation for gases transport in shale nanochannels: Helium, nitrogen, methane, and helium-methane mixture. Chem Eng J, 472: 144939.

Tade M D. 1967. Helium storage in Cliffside Field. J Petrol Technol, 19: 885–888.

Dan Y, Yan J F. Bao S J, Liang N, Ma L, Nie G Q, Cao J F, Ji S C, Han K. 2023. Discovery of Sinian-Cambrian multi-tier shale gas in Guidandi-1 well of southwest margin of Xuefeng uplift (in Chinese). Geol China, 50: 291–292.

Tao M X, Xu Y C, Shen P, Liu W H. 1997. Tectonic and geochemical characteristics and reserved conditions of a mantle source gas accumulation zone in eastern China. Sci China Ser D-Earth Sci, 40: 73–80.

Tao X W, Li J Z, Zhao L B, Li L W, Zhu W P, Xing L T, Su F Q, Shan X Q, Zheng H J, Zhang L P. 2019. Helium resources and discovery of first supergiant helium reserve in China: Hetianhe gas field (in Chinese). Earth Sci, 44: 1024-1041.

Tedesco S A. 2022. Geology and Production of Helium and Associated Gases. DOI: 10.1016/C2020-0-02538-7.

Torgersen T, O'Donnell J. 1991 The degassing flux from the solid Earth—release by fracturing. Geophys Res Lett, 18: 951–954.

Trull T W, Kurz M D, Jenkins W J. 1991. Diffusion of cosmogenic ^3He in olivine and quartz: Implications for surface exposure dating. Earth Planet Sci Lett, 103: 241–256.

USGS. Mineral Commodity Summaries 2023. U.S. Department of the Interior, U.S. Geological Survey, 2023.

Wang D F. 2020. CBM Geological Features and Resource Potential in Southwestern Margin of Jinzhong Basin (in Chinese). Coal Geol China, 32: 33–39.

Wang J, Jia H C, Tao C, Zhao Y Q, An C, Ma L B, Sun X, Dong Q W, Wang F B. 2023. Source and enrichment regularity of helium in Dongsheng Gas Field of Hangjinqi area, Ordos Basin (in Chinese). Nat Gas Geosci, 34: 566–575.

Wang X F, Liu Q Y, Liu W H, Zhang D D, Li X F, Zhan D. 2022. Accumulation mechanism of mantle-derived helium resources in petroliferous basins, eastern China. Sci China Earth Sci, 65: 2322–2334.

Wang Z C, Zhao W Z, Hu S Y, Xu A N, Jiang Q C, Jiang H, Huang S P, Li Q F. 2017. Control of tectonic differentiation on the formation of large oil and gas fields in craton basins: A case study of Sinian-Triassic of the Sichuan Basin (in Chinese). Nat Gas Ind, 37: 9–23.

Wang Z M, Wang Q H, Zhao M J, Li Y, Xu Z M. 2007. Geochemical characteristics and accumulation process of natural gas in Hetianhe gas field, Tarim Basin (in Chinese). Sci China Ser D-Earth Sci, 37(SII): 69–79.

Weinlich F H, Bräuer K, Kämpf H, Strauch G, Tesař J, Weise S M. 1999. An active subcontinental mantle volatile system in the western Eger rift, Central Europe: Gas flux, isotopic (He, C, and N) and compositional fingerprints. Geochim Cosmochim Acta, 63: 3653–3671.

Wilhelm E, Battino R, Wilcock R J. 1977. Low-pressure solubility of gases in liquid water. Chem Rev, 77: 319–262.

Wolf R A, Farley K A, Silver L T. 1996. Helium diffusion and low-temperature thermochronometry of apatite. Geochim CosmochimActa, 60(21): 4231–4240.

Wu K L, Chen Z X, Li X F, Xu J Z, Li J, Wang K, Wang H, Wang S H, Dong X H. 2017. Flow behavior of gas confined in nanoporous shale at high pressure: Real gas effect. Fuel, 205: 172–183.

Wu X, Li D, Han J, Zhu X X, Huang C, Cao Z C, Chang J, Liu Y C. 2022. Characteristics of present ultra-deep geothermal field in the northern Shuntuoguole low uplift, Tarim Basin (in Chinese). Acta Petro Sin, 43: 29–40.

Wu X Q, Dai J X, Liao F R, Huang S P. 2013. Origin and source of CO_2 in natural gas from the eastern Sichuan Basin. Sci China Earth Sci, 56(08): 1308–1317.

Xu C G. 2022. New progress and breakthrough directions of oil and gas exploration in China offshore area (in Chinese). China Offshore Oil Gas, 34: 9–16.

Xu S, Nakai S, Wakita H, Xu Y C, Wang X B. 1995. Helium isotope compositions in sedimentary basins in China. Appl Geochem, 10: 643–656.

Xu S, Zheng G D, Wang X B, Wang H L, Nakai S, Wakita H. 2014. Helium and carbon isotope variations in Liaodong Peninsula, NE China. J Asian Earth Sci, 90: 149–156.

Xu S, Zheng G D, Zheng J J, Zhou S X, Shi P L. Mantle-derived helium in foreland basins in Xinjiang, Northwest China. Tectonophysics, 2017, 694: 319-331.

Xu Y C, Shen P, Liu W H, Tao M X, Sun M L, Du J G. 1998. Geochemistry of noble gases in natural gas (in Chinese). Beijing: Science Press.

Xu Y C, Shen P, Tao M X, Liu W H. 1996. Geochemistry of mantle-derived volatile components in natural gas in the eastern oil and gas region: A new type of helium resources: Industrial storage of mantle-derived helium in sedimentary shells (in Chinese). Sci China Ser D-Earth Sci, 26: 1–8.

Xu Y C, Shen P, Tao M X, Sun M L. 1990. Industrial storage of mantle-derived helium and Tan-Lu Fault Zone (in Chinese). Chin Sci Bull, 12: 932–935.

Xu Y C. 1997. Helium isotope distribution of natural gasses and its structural setting (in Chinese). Earth Sci Front, 4: 185–190.

Xu Y C, Shen P, Tao M X, Liu W H. 1997a. Geochemistry on mantle-derived volatiles in natural gases from eastern China oil/gas provinces (I). Sci China Ser D-Earth Sci, 40: 120–129.

Xu Y C, Shen P, Tao M X, Liu W H. 1997b. Geochemistry on mantle-derived volatiles in natural gases from eastern China oil/gas provinces (II). Sci China Ser D-Earth Sci, 40: 315–321.

Xu Y C, Shen P, Tao M X, Sun M L. 1994. Distribution of the helium isotopes in natural gases from oil-gas-bearing basins in China. Chinese Sci Bull, 39: 1905–1911.

Yakutseni V P. 2014. World helium resources and the perspectives of helium industry development. Petroleum Geology-Theoretical and Applied Studies, 9: 1–22.

Yang F Z, Wang J Y, Pan Q B. 1991. Discussion on origin of Upper Neogene helium-rich gases in Huangqiao, North Jiangsu (in Chinese). Oil Gas Geol, 12: 340–345.

Yu Q X, Shi Z, Wang D G, Guo H. 2013. Analysis on helium enrichment characteristics and reservoir forming conditions in Northwest Tarim Basin (in Chinese). Northwest Geol, 46: 215–222.

Zeng H, Li J, Huo Q. 2013. A review of alkane gas geochemistry in the Xujiaweizi fault-depression, Songliao Basin. Mar Petrol Geol, 43: 284–296.

Zhang Q, Zhou J L, Li Y H, Chen G C, Wei J S, Guo W. 2022. The occurrence state and restraint factors of helium-produced elements (U, Th) in the granites from the southern margin of Weihe Basin: Evidences from Huashan complex (in Chinese). Northwest Geol, 55: 241–256.

Zhang T W, Zhang M, Bai B J, Wang X B, Li L W. 2008. Origin and accumulation of carbon dioxide in the Huanghua depression, Bohai Bay Basin, China. AAPG Bull, 92: 341–358.

Zhang W, Li Y H, Zhao F H, Han W, Li Y, Wang Y P, Holland G, Zhou Z. 2019a. Using noble gases to trace groundwater evolution and assess helium accumulation in Weihe Basin, central China. Geochim Cosmochim Acta, 251: 229–246.

Zhang W, Li Y H, Zhao F H, Han W, Zhou J L, Holland G, Zhou Z. 2019b. Quantifying the helium and hydrocarbon accumulation processes using noble gases in the North Qaidam Basin, China.

Chem Geol, 525: 368–379.

Zhang W. 2019. Study on reservoir formation mechanism of strategic helium resources in the northern margin of Guanzhong and Qaidam (in Chinese). Beijing：China University of Mining and Technology (Beijing).

Zhang X B, Zhou F, Cao Z Y, Liang M L. 2020. Finding of the Dongping economic Helium gas field in the Qaidam Basin, and Helium source and exploration prospect (in Chinese). Nat Gas Geosci, 31: 1585–1592.

Zhao G P. 2017. Characterization of fluid inclusions and timing of gas accumulation in Upper Paleozoic reservoirs of Hangjinqi area, Ordos Basin (in Chinese). Oil Gas Geol, 38: 905–912.

Zhao W Z, Li J Z, Yang T, Wang S F, Huang J L. 2016. Geological difference and its significance of marine shale gases in South China (in Chinese). Petrol Explor Dev, 43: 499–510.

Zhao Y Q, Ni C H, Wu X Q, Zhu J H, Liu G X, Wang F B, Jia H C, Zhang W, Qi R, An C. 2022. Geochemical characteristics and source of Permian formation water in Hangjinqi area, Ordos Basin (in Chinese). Petrol Geol Exp, 44: 279–287.

Zhao Y X, Zhang Y, Li C L. 2012. Analysis of Supply and Price System for Global Helium Gas (in Chinese). Chem Propell Polym Mat,10: 91–96.

Zheng L, Wang S, Liao Y, Feng Z. 2001. CO_2 gas pools in Jiyang Sag, China. Appl Geochem, 16: 1033–1039.

Zhong K, Zhu W L, Xue Y A, Zhou X H, Xu C G, Niu C M. 2019. Petroleum geologic conditions and distributional features of large-and medium-sized oil and gas fields in Bohai Sea Basin (in Chinese). Oil Gas Geol, 40: 92–100.

Zhong X. 2017. Distribution characteristics and control factors of helium gas in northern Songliao Basin (in Chinese). Geol Surv Res, 40: 300–305.

Zhou X Y, Yang H J, Li Y, Wang Y H, Zeng C M. 2006. Cases of discovery and exploration of marine fields in China (Part 7): Hotanhe Gas Field in Tarim Basin (in Chinese). Mar Origin Petrol Geol, 11: 55–62.

Zhou Z, Ballentine C J, Kipfer R, Schoell M, Thibodeaux S. 2005. Noble Gas Tracing of Groundwater/coalbed Methane Interaction in the San Juan Basin, USA. Geochim Cosmochim Acta, 69: 5413–5428.

Zhu R X, Xu Y H. 2019. The subduction of the west Pacific plate and the destruction of the North China Craton (in Chinese). Sci China Earth Sci, 49: 1346–1356.